

AD A068257

DDC FILE COPY

LEVEL *12*

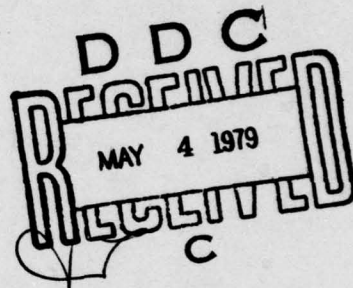


RADC-TR-79-35
Final Technical Report
March 1979

STUDY OF RESONANT LOSS FOR HELIX TWTs

Varian Associates, Inc.

C. E. Hobrecht



APPROVED FOR PUBLIC RELEASE; DISTRIBUTION UNLIMITED

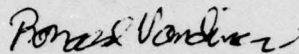
ROME AIR DEVELOPMENT CENTER
Air Force Systems Command
Griffiss Air Force Base, New York 13441

79 05 03 007

This report has been reviewed by the RADC Information Office (OI) and is releasable to the National Technical Information Service (NTIS). At NTIS it will be releasable to the general public, including foreign nations.

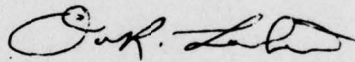
RADC-TR-79-35 has been reviewed and is approved for publication.

APPROVED:



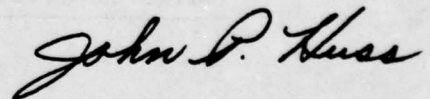
RONALD VANDIVIER
Project Engineer

APPROVED:



OWEN R. LAWTER
Colonel, USAF
Chief, Surveillance Division

FOR THE COMMANDER:



JOHN P. HUSS
Acting Chief, Plans Office

If your address has changed or if you wish to be removed from the RADC mailing list, or if the addressee is no longer employed by your organization, please notify RADC (OCTP) Griffiss AFB NY 13441. This will assist us in maintaining a current mailing list.

Do not return this copy. Retain or destroy.

*MISSION
of
Rome Air Development Center*

RADC plans and conducts research, exploratory and advanced development programs in command, control, and communications (C³) activities, and in the C³ areas of information sciences and intelligence. The principal technical mission areas are communications, electromagnetic guidance and control, surveillance of ground and aerospace objects, intelligence data collection and handling, information system technology, ionospheric propagation, solid state sciences, microwave physics and electronic reliability, maintainability and compatibility.



UNCLASSIFIED

SECURITY CLASSIFICATION OF THIS PAGE (When Data Entered)

19 REPORT DOCUMENTATION PAGE		READ INSTRUCTIONS BEFORE COMPLETING FORM	
1. REPORT NUMBER RADC-TR-79-35	2. GOVT ACCESSION NO.	3. RECIPIENT'S CATALOG NUMBER	
4. TITLE (and Subtitle) STUDY OF RESONANT LOSS FOR HELIX TWTs.		5. TYPE OF REPORT & PERIOD COVERED Final Technical Report. 1 Sep 77 - 1 Sep 78	
7. AUTHOR(s) C. E. Hobrecht		6. PERFORMING ORG. REPORT NUMBER N/A	
9. PERFORMING ORGANIZATION NAME AND ADDRESS Varian Associates, Inc. 611 Hansen Way Palo Alto CA 94303		8. CONTRACT OR GRANT NUMBER(s) F30602-77-C-0172	
11. CONTROLLING OFFICE NAME AND ADDRESS Rome Air Development Center (OCTP) Griffiss AFB NY 13441		10. PROGRAM ELEMENT, PROJECT, TASK AREA & WORK UNIT NUMBERS 62702F 55730222	
14. MONITORING AGENCY NAME & ADDRESS (if different from Controlling Office) Same		12. REPORT DATE March 1979	
		13. NUMBER OF PAGES 68	
		15. SECURITY CLASS. (of this report) UNCLASSIFIED	
		15a. DECLASSIFICATION/DOWNGRADING SCHEDULE N/A	
16. DISTRIBUTION STATEMENT (of this Report) Approved for public release; distribution unlimited			
17. DISTRIBUTION STATEMENT (of the abstract entered in Block 20, if different from Report) Same			
18. SUPPLEMENTARY NOTES RADC Project Engineer: Ronald Vandivier (OCTP)			
19. KEY WORDS (Continue on reverse side if necessary and identify by block number) Helix Traveling Wave Tube Resonant Loss TWT Resonator Backward Wave Oscillation BWO			
20. ABSTRACT (Continue on reverse side if necessary and identify by block number) One of the most effective techniques for eliminating backward wave oscillations (BWOs) in helix type traveling wave tubes (TWTs) is resonant loss. The fundamental purpose of this program was to perform experimental work which would give a more complete understanding of the electrical and mechanical characteristics of this BWO suppression scheme. In order to accomplish this, the following data were obtained: resonant frequencies for a broad range of resonator geometries, resonator materials for high Q and high loss, frequency limits, (Cont'd)			

DD FORM 1 JAN 73 1473

EDITION OF 1 NOV 65 IS OBSOLETE

UNCLASSIFIED

SECURITY CLASSIFICATION OF THIS PAGE (When Data Entered)

364100

Sw

007

UNCLASSIFIED

SECURITY CLASSIFICATION OF THIS PAGE(When Data Entered)

Item 20 (Cont'd)

Cont. → achievable peak RF power levels for tubes using this scheme, in-band effects, frequency characteristics (Q), effects of asymmetric arrangements, power handling capability, and the effects of temperature and temperature cycling. Probably the most important conclusions are two: high power, PPM focused, conduction cooled helix TWTs using resonant loss for BWO suppression are no longer limited in achievable peak RF output power due to BWO and such tubes can, for the first time since their invention, be designed solely for the desired in-band RF performance. The latter conclusion is a direct result of the fact that the in-band effects of resonant loss are minimal. Also presented are two fabrication methods: lift - off and acid etching. Either method can be used to fabricate resonators composed of titanium and gold, the first metal being present to assure that the resonators adhere to the boron nitride substrate. This composition possesses excellent electrical and mechanical properties. Limited stress test results are presented which demonstrate the latter.

ACCESSION for	
NTIS	White Section <input checked="" type="checkbox"/>
DDC	Buff Section <input type="checkbox"/>
UNANNOUNCED	<input type="checkbox"/>
JUSTIFICATION	
BY	
DISTRIBUTION/AVAILABILITY CODES	
Dist.	Avail. and SPECIAL
A	

UNCLASSIFIED

SECURITY CLASSIFICATION OF THIS PAGE(When Data Entered)

TECHNICAL SUMMARY

One of the most effective techniques for eliminating backward wave oscillations (BWOs) in helix type traveling wave tubes (TWTs) is resonant loss. The fundamental purpose of this program was to perform experimental work which would give a more complete understanding of the electrical and mechanical characteristics of this BWO suppression scheme. In order to accomplish this, the following areas were investigated:

DETERMINATION OF RESONATOR GEOMETRY

Measurements of the resonant frequencies of a wide range of resonator geometries were made. The resulting data allow the accurate determination of a resonator geometry for a desired resonant frequency. In this same section, two techniques for fabricating resonant loss on boron nitride are described: lift-off and acid etching.

OPTIMUM RESONATOR MATERIALS

The optimum resonator materials from both a mechanical and electrical viewpoint appear to be a combination of titanium-gold. The titanium is first sputtered onto the substrate in a very thin layer so that the following, much thicker layer of gold, which is also sputtered, can adhere to this substrate. This combination adheres well and produces lossy resonators with sharp loss characteristics.

FREQUENCY LIMITATIONS

With the fabrication techniques described above, resonant loss can be fabricated up to approximately 30 GHz on boron nitride. Above this frequency, beryllia appears to be the desired substrate material.

ACHIEVABLE PEAK RF POWER

The output power of helix TWTs built using resonant loss for BWO stability is not limited by BWO, since resonant loss provides high loss densities. During this program a ten kilowatt peak power tube was built. It operated from 3 to 6 GHz and was unconditionally stable.

COMPATIBLE DISTRIBUTED LOSS

If both resonant and distributed loss are to be placed on a helix support rod, the latter can be applied by spraying colloidal carbon, rf sputtering molybdenum or tungsten carbide on the broad face of the rod opposite the resonant loss. Another approach is to place resonant loss on one or two of the helix support rods and distributed loss on the remaining rod(s).

IN-BAND EFFECTS

If the ratio of the helix-resonator separation to the average helix diameter lies between 0.03 and 0.04, resonant loss typically decreases the circuit phase velocity by 7% and 10% at the lower and upper band edge frequencies respectively. If the circuit pitch is increased to compensate for the resonant loss, the interaction impedance is unchanged at the lower band edge and is reduced by 7% to 15% at the upper band edge. Each of these quantities assumes that the resonant loss introduces little or no loss into the operating band.

FREQUENCY CHARACTERISTICS (Q)

The frequency response of resonant loss combined with typical helix circuit characteristics, specifically the frequency separation between the upper band edge and the BWO frequency, imply that resonant loss typically introduces the following amounts of loss at the upper band edge: E-F band, no loss; G-H band, 3 dB; and I-J band, 10 dB. These values assume that resonant loss is placed on all three support rods, between each helix turn, over typical output circuit lengths for each frequency band.

ASYMMETRY EFFECTS

If resonant loss is placed on only one or two support rods, a stopband centered at the π phase shift frequency is introduced. Since this stopband increases the loss at this frequency, such asymmetric arrangements appear to be beneficial. Several tubes have been built with such asymmetric resonant (and distributed) loss, and they have been unconditionally stable.

POWER HANDLING CAPABILITY

A single resonator can absorb at least ten watts of CW power without being destroyed. It is felt that this level is far in excess of the actual power levels encountered in typical applications.

TEMPERATURE EFFECTS

The resonant frequency of a resonator decreases slightly with temperature. A limited amount of temperature cycling, between 60°C and 200°C, indicates that the resonators are mechanically sound.

Finally, it should be emphasized that resonant loss gives the circuit designer the freedom to design the circuit solely for in-band performance, since resonant loss has only very slight in-band effects.

TABLE OF CONTENTS

<u>Section</u>	<u>Page</u>
I. INTRODUCTION.....	1
A. Program Plan.....	1
B. Resonant Loss -- What Is It and Why Is It Needed?.....	2
II. DETERMINATION OF RESONATOR GEOMETRY.....	7
A. Mapping Experiment.....	7
B. Fabrication Techniques.....	10
1. Lift-Off Process.....	11
2. Acid-Etching Process.....	11
III. OPTIMUM RESONATOR MATERIALS.....	15
IV. FREQUENCY LIMITATIONS.....	16
V. ACHIEVABLE PEAK RF POWER.....	18
A. Peak Power Limits.....	18
B. High Peak Power TWT.....	21
VI. COMPATIBLE DISTRIBUTED LOSS.....	36
A. Pyrolytic Deposition.....	36
B. Colloidal Carbon.....	36
C. Sputtered Films.....	36
D. Low Q Resonant Loss.....	37
VII. IN-BAND EFFECTS OF RESONANT LOSS.....	38
VIII. FREQUENCY CHARACTERISTICS (Q).....	46
IX. ASYMMETRY EFFECTS.....	49
X. POWER HANDLING CAPABILITY.....	52
XI. TEMPERATURE EFFECTS.....	53
XII. CONCLUDING REMARKS.....	54
XIII. SUGGESTIONS FOR FURTHER WORK.....	55
REFERENCES.....	56

LIST OF ILLUSTRATIONS

<u>Figure</u>		<u>Page</u>
1.	Helix TWT Circuit with Resonant Loss on Support Rod.....	3
2.	Insertion Loss vs Frequency of Helix Slow Wave Circuit with and without Resonant Loss.....	4
3.	Electric Field Configurations for a Helix and Resonator at the Frequency Corresponding to a Phase Shift of π Radians per Helix Turn.....	6
4.	Resonator Geometry.....	8
5.	Results of Mapping Experiment.....	9
6.	Lift-Off Process.....	12
7.	Acid Etching Process.....	13
8.	Peak Output Power Limits for Helix TWTs in 1974.....	19
9.	Peak Output Power Limits Other Than BWO for Helix TWTs in 1976.....	20
10.	Ten Kilowatt TWT Slow Wave Circuit.....	22
11.	BWO Start Current Calculations.....	23
12.	Measured Resonant Loss Characteristic.....	25
13.	Comparison of Calculated (Without Resonant Loss) and Measured (With Resonant Loss) Phase Velocity.....	26
14.	Comparison of Calculated (Without Resonant Loss) and Measured (With Resonant Loss) Interaction Impedance.....	27
15.	Calculated Small Signal Gain.....	29
16.	Magnetic Circuit.....	30
17.	Ten Kilowatt TWT.....	31
18.	Measured Saturated Output Power vs Frequency.....	32
19.	Measured Saturated Gain vs Frequency.....	33
20.	Measured Small Signal Gain vs Frequency.....	34
21.	Measured Insertion Loss of Three Inch Length of G-H Band Circuit with Resonant Loss.....	40

LIST OF ILLUSTRATIONS (Cont.)

<u>Figure</u>		<u>Page</u>
22.	Phase Velocity vs Frequency for Circuits with and without Resonant Loss.....	41
23.	Impedance vs Frequency for Circuits with and without Resonant Loss.....	42
24.	Phase Velocity vs Frequency for Circuits with and without Resonant Loss.....	43
25.	Impedance vs Frequency for Circuits with and without Resonant Loss.....	44
26.	Insertion Loss vs Frequency of I-J Band Circuit with Resonant Loss.....	47
27.	Measured Insertion Loss vs Frequency for G-H Band Circuit with One Resonant Loss Rod.....	50
28.	Insertion Loss vs Frequency for G-H Band Circuit with Two Resonant Loss Rods.....	51

EVALUATION

A 10 KW peak power TWT was designed to operate over the frequency range of 3 to 6 GHz. Measurements were taken at a duty cycle of 0.1% and with a 10 usec pulsewidth. The 10 KW tube has demonstrated that wideband helix traveling wave tubes need no longer be limited to peak power levels of several kilowatts because of backward wave oscillations. Resonant loss can be credited with the responsibility for the successful elimination of this major limitation. It would appear that peak power levels in excess of 100 KW are possible for PPM focused helix TWTs using resonant loss as the sole method of BWO suppression.

Ronald Vandivier

RONALD VANDIVIER
Proj Engr/OCTP

I. INTRODUCTION

A. PROGRAM PLAN

One of the most effective techniques for eliminating backward wave oscillations (BWOs) in helix type traveling wave tubes (TWTs) is resonant loss (Reference 1). The fundamental purpose of this program was to perform experimental work which would give a more complete understanding of the electrical and mechanical characteristics of this BWO suppression scheme. In order to accomplish this, the following areas were investigated:

Determination of Resonator Geometry: What resonator geometry can both fit in the available space on the helix rod and resonate at the desired frequency? Also, how does one reliably fabricate these resonators using pyrolytic boron nitride as the substrate material?

Optimum Resonator Materials: Of which metal or metals should the resonators be composed in order to realize the desired electrical and mechanical characteristics, such as high loss (low reactance), high Q, good adhesion and long operating life?

Frequency Limitation: What is the highest frequency at which resonators can be reliably fabricated and provide the desired electrical characteristics, especially high Q?

Achievable Peak RF Power: What peak rf output powers can be achieved in unifilar helix TWTs which use only resonant loss for BWO suppression?

Compatible Distributed Loss: What techniques should be used to place both distributed and resonant loss on the same helix support rod?

In-Band Effects: What effects does resonant loss have on the in-band performance of a tube?

Frequency Characteristics (Q): What are the typical frequency response characteristics of resonators for use in E-F band through I-J band tubes? Are these characteristics sufficiently sharp, i.e., does resonant loss introduce enough loss at the BWO frequency to suppress oscillations and a low enough level in the operating band so that it does not degrade the tube's performance?

Asymmetry Effects: What are the effects of an asymmetric resonant loss arrangement, such as placing it on only one support rod?

Power Handling Capability: How much power can an individual resonator absorb before it is destroyed?

Temperature Effects: How does the resonant frequency change with temperature? How does temperature cycling influence the mechanical integrity of a resonator?

Clearly, many of these areas overlap and the subsequent discussions will emphasize this.

This report consists of thirteen sections. Following the introduction, the next ten sections (II through XI) answer the questions outlined above. Section XII provides some concluding remarks, and Section XIII provides suggestions for further work.

B. RESONANT LOSS -- WHAT IS IT AND WHY IS IT NEEDED?

Resonant loss is a relatively new BWO suppression technique for helix TWTs. It was invented at Varian Associates, Inc. in 1976. In its present form, it consists of lossy, open circuited meander lines placed on the broad face of each helix support rod between each helix turn. Figure 1 shows a photograph of a helix and one of its support rods with resonant loss on it.

The geometry of a "resonator" is chosen so that it resonates at the tube's BWO frequency. Ideally it would provide no loss in the tube's operating band and great loss at this frequency. The frequency response of a typical resonator is shown in Figure 2. Shown here is the insertion loss of a length

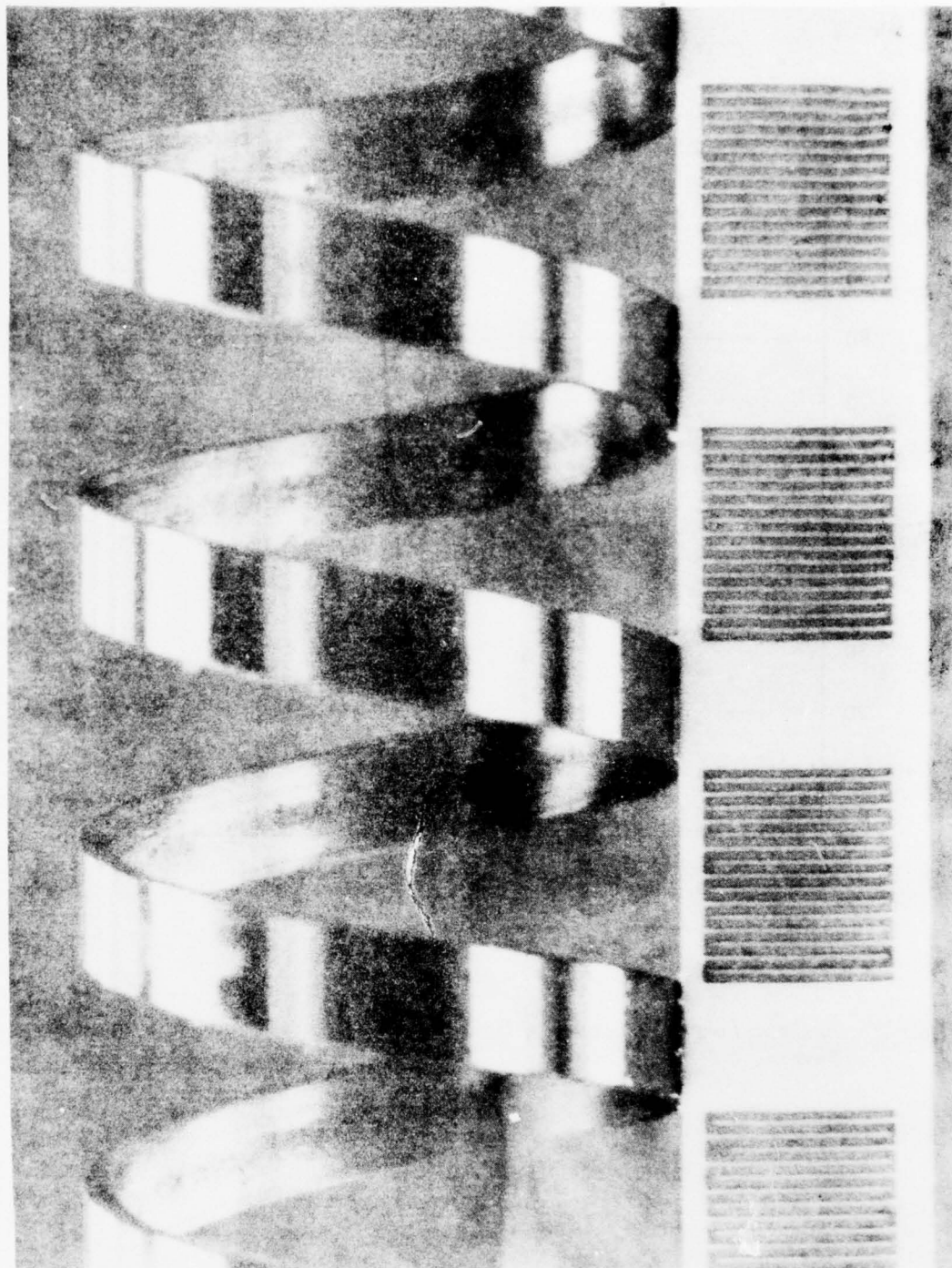


Figure 1. Helix TWT Circuit with Resonant Loss on Support Rod

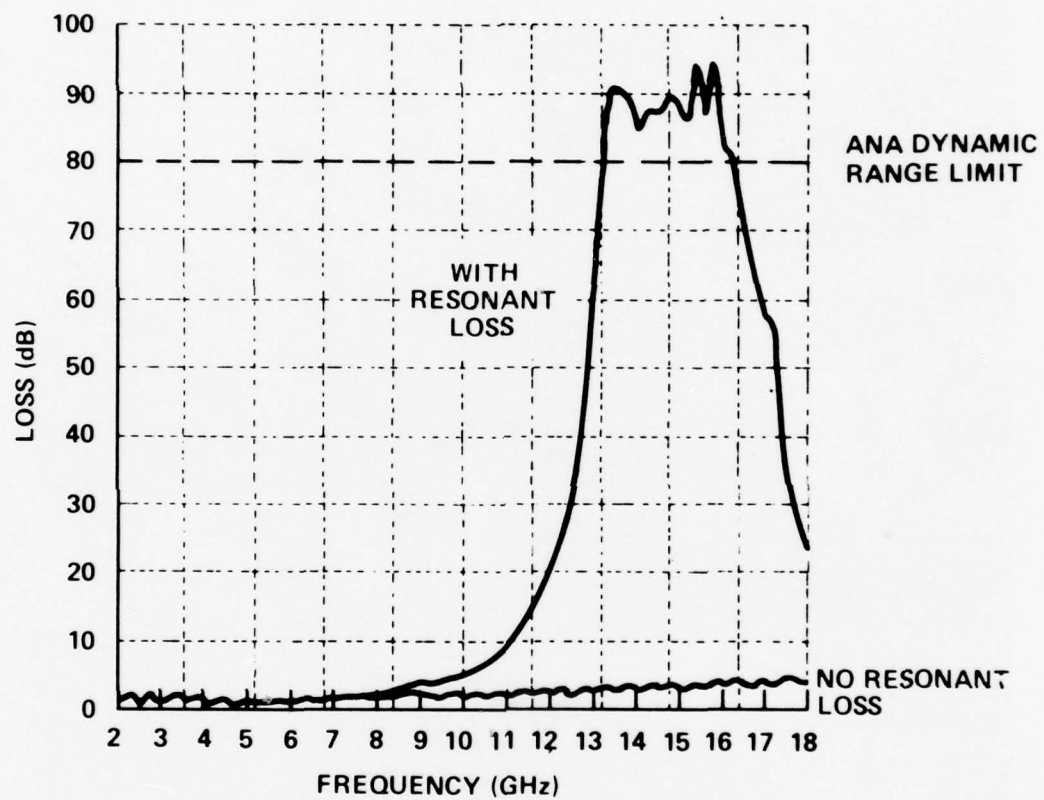


Figure 2. Insertion Loss vs Frequency of Helix Slow Wave Circuit with and without Resonant Loss

of G-H-I band helix circuit both without and with resonant loss. The departure from the ideal loss characteristic can be seen: The resonator introduces several decibels of loss at the tube's upper operating band edge frequency, 10 GHz.

Figure 3 shows the electric field configuration for a helix slow wave circuit at a frequency corresponding to a phase shift per helix pitch of π -radians. This frequency is close to the BWO frequency. Also shown is the field distribution for a meander line printed on the support rod at its resonant frequency. The parallelism of the helix's and meander line's field configurations gives rise to strong coupling between them. As a result, there is a transfer of energy from the helix to the meander line at the latter's resonant frequency. In this manner, circuit loss is provided at and near the BWO frequency and, if it is sufficient, backward wave interaction in this region is suppressed.

Resonant loss is a very effective BWO suppression technique because very large amounts of loss can be introduced at and near the BWO frequency, while little loss is introduced in the operating band. The achievable loss densities at oscillation frequencies lie between 2 and 3 dB per helix turn per rod, depending on the circuit geometry. For example, it is easy to incorporate over 100 dB of loss at the oscillation frequency (with only 2 dB of loss in the operating band) into the output section of a high-power TWT operating in G-H-I band.

The resonant circuits are deposited on the support rods using standard microwave integrated circuit techniques. These techniques will be fully explained in Section II.

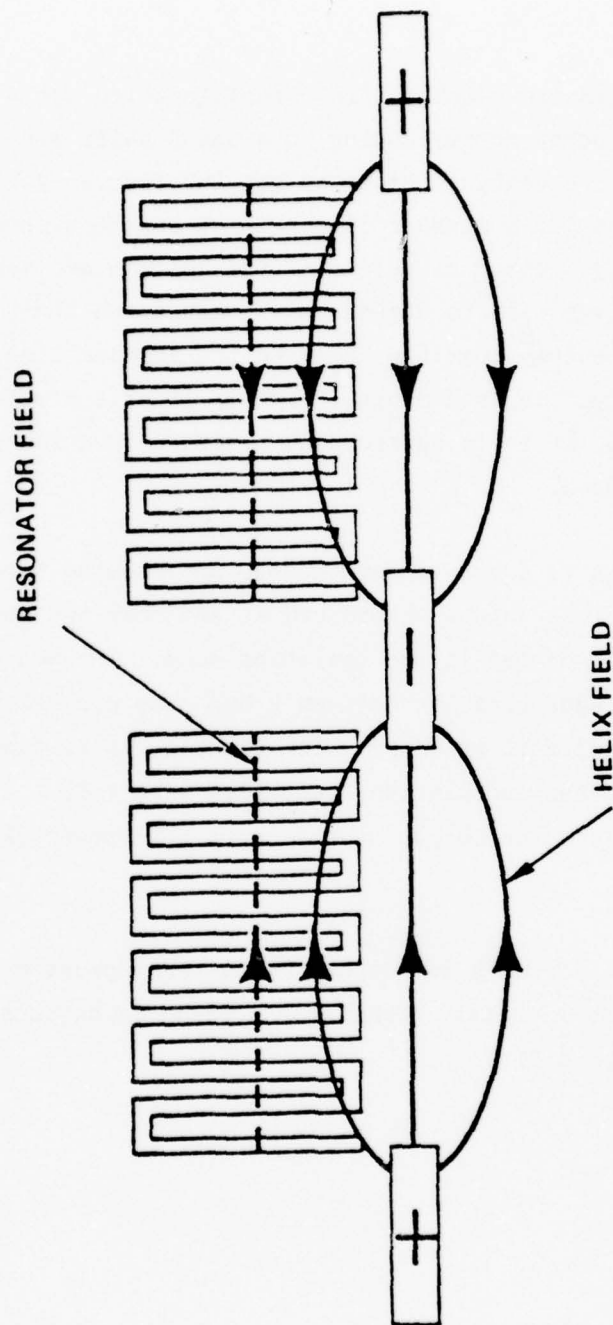


Figure 3. Electric Field Configurations for a Helix and Resonator at the Frequency Corresponding to a Phase Shift of π Radians per Helix Turn

II. DETERMINATION OF RESONATOR GEOMETRY

A. MAPPING EXPERIMENT

The resonator geometry must be chosen so that the resonator can fit into the available space on the rod and resonate at the desired frequency. Generally, the "desired" frequency is the one which results in little or no loss being introduced into the tube's operating band, while sufficient loss is introduced at the BWO frequency to stabilize the tube. The amount of loss needed at this frequency can be predicted by performing start oscillation current calculations. Examples of such calculations are given in Section V.

Early in the program, attempts to solve the meander line boundary value problem were made. The solutions obtained, however, did not correlate well with measured data. In light of the complexity of the problem, this was not surprising. As a result, it was decided to resort to an experimental approach.

A "mapping" experiment was performed. Basically, resonator geometries, whose dimensions bracketed all possible future designs, were fabricated and their resonant frequencies measured. The standard resonator geometry is shown in Figure 4.

Thus, five different pattern widths (W) were used: 0.015", 0.020", 0.030", 0.040", and 0.050". For each width, two different line widths (T) were used. For each pattern width and line width, the unwrapped length (L) was varied over a large range by varying the number of "loops" (N). Each resonator pattern was fabricated on a pyrolytic boron nitride substrate of two different thicknesses. The resonant frequencies were measured in a transmission type fixture, whose helix diameter was made sufficiently small so that its π phase shift frequency was higher than the highest resonant frequency to be measured. To measure a particular resonator pattern, the insertion loss of the fixture with three loss-free (no resonant or distributed loss) rods was first measured. Then one of the three rods was replaced by one on which resonant loss was

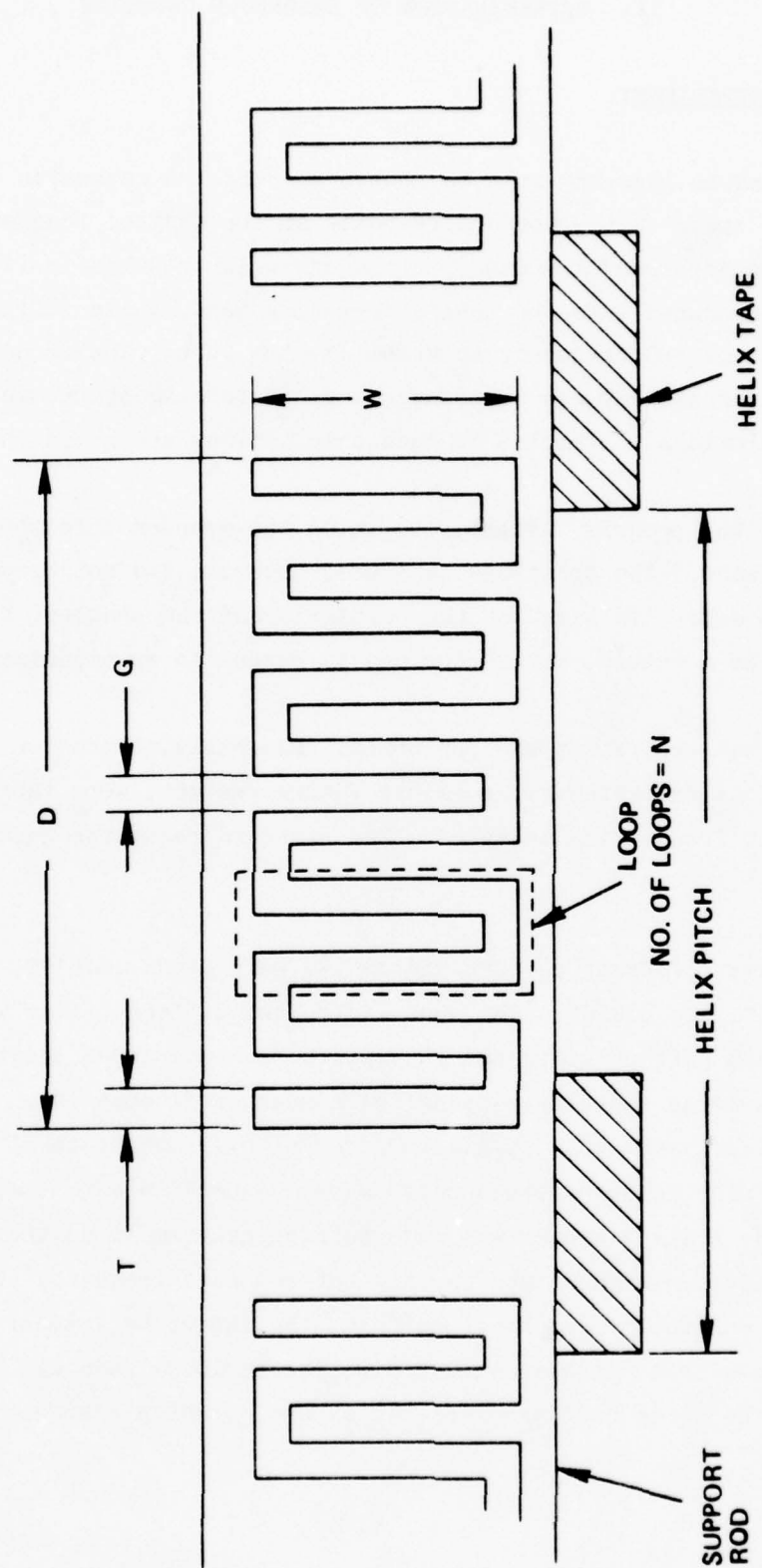


Figure 4. Resonator Geometry

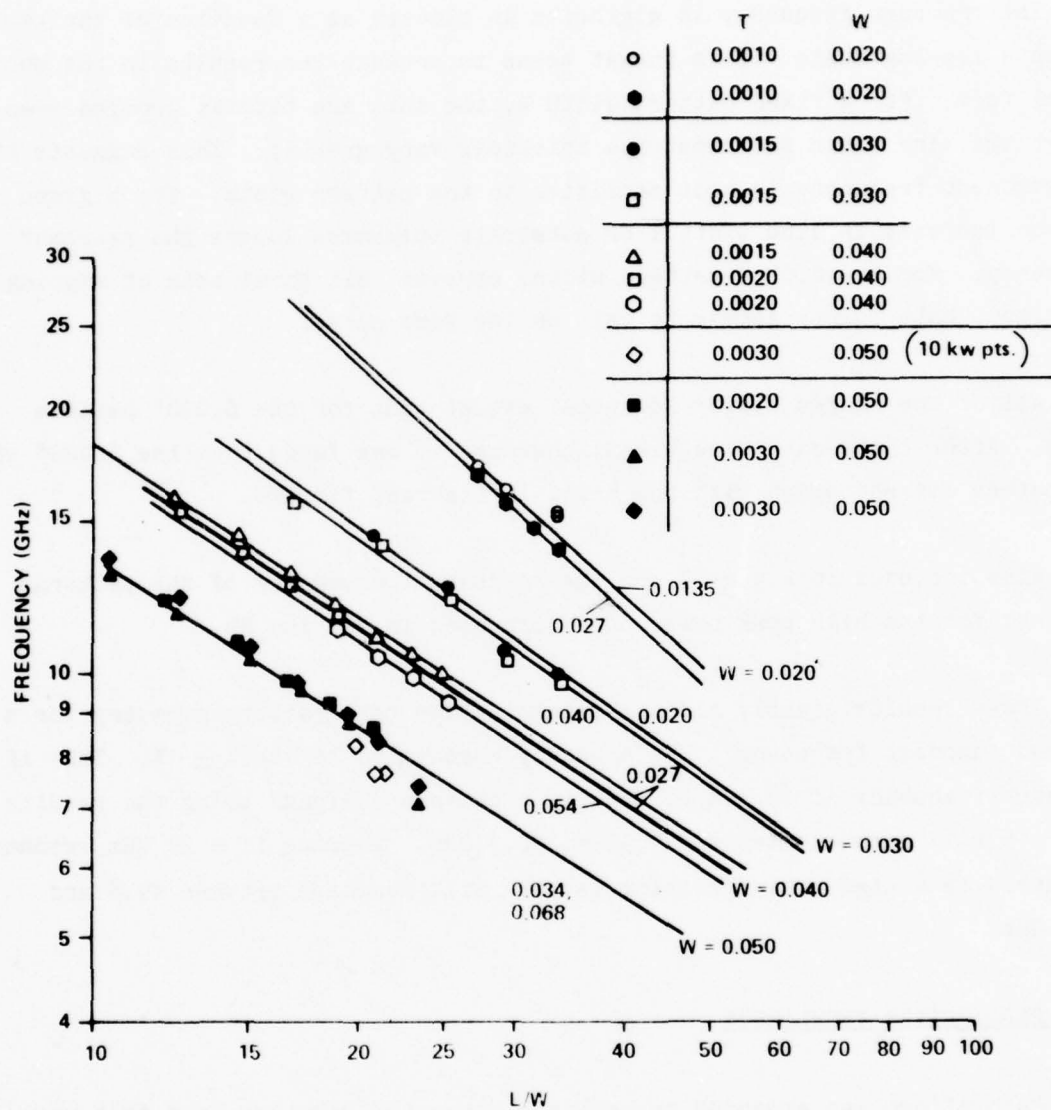


Figure 5. Results of Mapping Experiment

deposited, and the insertion loss of the assembly was remeasured. The results of the mapping experiment are shown in Figure 5.

The resonant frequency in gigahertz is plotted as a function of the ratio L/W on a log-log scale. This format seems to present the results in the most useful form. For a fixed pattern width W , the data are tightly grouped even though the line width and substrate thickness vary greatly. This suggests that the resonant frequency is most sensitive to the pattern width. For a given L/W , an increase in line width T or substrate thickness lowers the resonant frequency. For the 0.050" pattern width, however, all three sets of mapping experiment data points appear to fall on the same curve.

All of the shapes appear identical except that for the 0.020" pattern width. After these data were taken, however, it was found that the 0.020" wide resonators did not align with the helix in the test fixture.

Also included in Figure 5 are the resonant frequencies of the patterns designed for the high peak power tube discussed in Section VB.

These results greatly aid the determination of a pattern geometry for a desired resonant frequency. The accuracy appears to be about $\pm 1\%$. Thus if a resonant frequency of 10 GHz is sought, a pattern designed using the results of Figure 5 will resonate between 9.9 and 10.1 GHz. Whereas if a 20 GHz resonant frequency is wanted, the resulting pattern will resonate between 19.8 and 20.2 GHz.

B. FABRICATION TECHNIQUES

Much effort was expended to reliably fabricate resonant loss on boron nitride. In fact, at the start of the program, resonators simply could not be made to adhere to this substrate.

During the course of the program, two fabrication procedures were developed: lift-off and acid-etching. Although each of these is standard microwave integrated circuit fabrication techniques, they necessarily required refinement

for the present work, due to the unique physical properties of boron nitride and the large substrate sizes involved.

In general, the lift-off method is easier to implement than the acid-etching method, and it avoids the need for messy and toxic acids. For this reason, it is presently the preferred method of fabrication. Before the actual fabrication process, the substrate must be lapped and chemically cleaned.

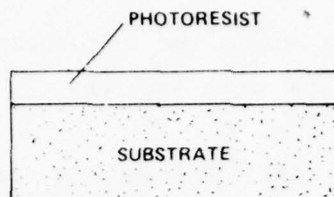
1. Lift-Off Process

The five steps of the lift-off process are shown in Figure 6. The substrate is first coated with positive photoresist. The photomask containing the resonator patterns as clear images is then placed in intimate contact with the coated substrate. Ultraviolet light passes through the clear portions of the mask and chemically changes the photoresist, so that it is soluble in the developing solution. A thin layer of titanium is first sputtered onto the substrate to improve the adhesion of the second film, a thick layer of gold. The gold should be at least two skin depths thick at the resonant frequency. Finally, the substrate is immersed in acetone to lift-off the excess photoresist and sputtered metals.

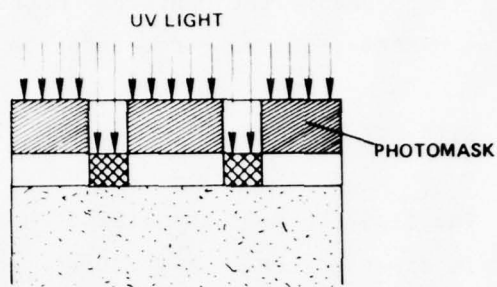
2. Acid-Etching Process

This process can be broken down into six steps, and these are shown in Figure 7. The cleaned and lapped substrate is coated with metals as in Step 4 of the lift-off method. Positive photoresist is then applied and exposed to ultraviolet light as before. In this case, the resonator pattern images are opaque. In Step 4, the exposed photoresist is developed, so that the only remaining photoresist is in the shape of the resonator patterns. The gold and titanium not lying under photoresist are removed using commercial etchants. If the etching is carefully controlled, the metals under the photoresist are only slightly attacked or undercut. In the final step, the remaining photoresist is removed with an acetone rinse.

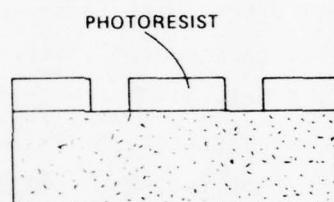
STEP 1 - COAT WITH PHOTORESIST



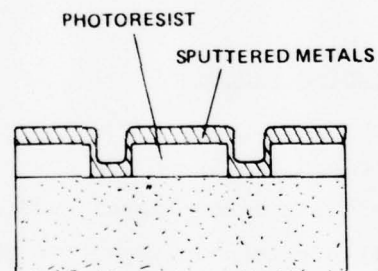
STEP 2 - EXPOSE



STEP 3 - DEVELOP



STEP 4 - SPUTTER



STEP 5 - LIFT-OFF

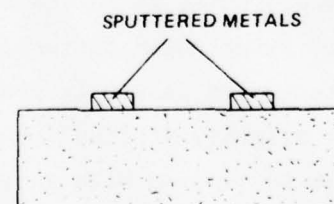
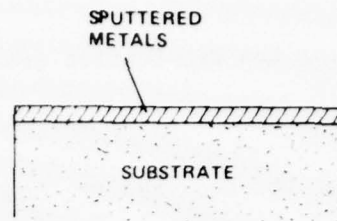
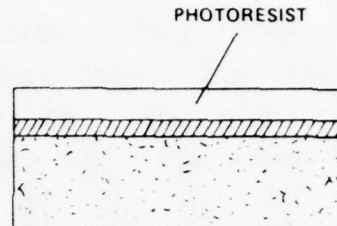


Figure 6. Lift-Off Process

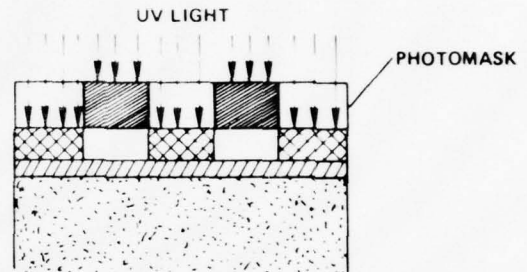
STEP 1 - SPUTTER



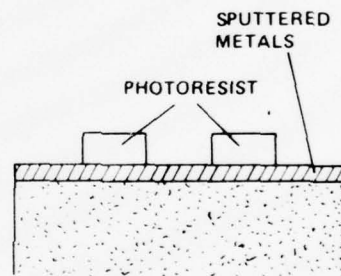
STEP 2 - COAT WITH PHOTORESIST



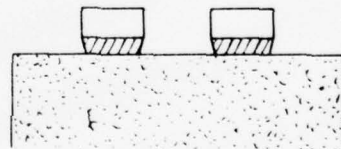
STEP 3 - EXPOSE



STEP 4 - DEVELOP



STEP 5 - ETCH



STEP 6 - REMOVE PHOTORESIST



Figure 7. Acid Etching Process

Following the fabrication process, the substrate is cut up into the individual support rods.

In order to check the resonant frequency of the resonators on these rods, a simple transmission test fixture can be constructed. The fixture is basically the slow wave circuit mounted in a split brass block with an rf window attached to each end of the helix. Two of the rods can be glued to the helix and block, leaving the third available for removal and replacement by a loss-free rod or a rod deposited with the resonant loss. In this way, the insertion loss of the helix with and without resonant loss can be measured (as in Figure 2).

III. OPTIMUM RESONATOR MATERIALS

The last section indicated that the currently preferred resonator materials are a titanium-gold combination. Each of these metals is sputtered onto the substrate. The titanium is used solely to make the gold adhere to the boron nitride. Zirconium has also been used as the adhesion layer with equal success. Since both metals are active, they adhere well to the boron nitride, thereby creating nucleation sites for physical bonding between themselves and the gold.

Gold was chosen as the bulk resonator material because of its good conductivity, oxidation resistance, and general ease of handling. Initially, it was thought that it might be too conductive, thereby making the resonators too reactive and not sufficiently lossy. This has not proven to be true, however. The approximately half a dozen tubes built and tested to date using titanium-gold or zirconium-gold resonators have been unconditionally BWO stable. A great deal of effort was expended to make titanium-gold resonators adhere to boron nitride, and eventually this was done. Thus, the titanium-gold combination appears to be both mechanically and electrically sound.

A limited number of resonators were fabricated using copper and silver as the bulk material, and each had the same loss characteristic (Q) as did the gold resonators.

IV. FREQUENCY LIMITATIONS

In discussing the frequency limitations of resonant loss, two areas should be addressed: fabrication and electrical characteristics.

Using the techniques of Section II, resonant loss can be reliably fabricated for any tube operating within the 2 to 18 GHz range. Thus, resonators which resonate as low as 5 GHz and as high as 23 GHz have been fabricated and incorporated into actual tubes. It would appear that resonators with resonant frequencies up to 30 GHz could be made rather straightforwardly using boron nitride as a substrate. At this frequency, the resonator line width would be about three-quarters of a mil (0.00075") or 19 microns. This frequency limit is due to the nature of the boron nitride surface. In order to obtain pattern definition for three-quarter mil lines, it would have to be polished to about a five microinch or better surface finish. Experience has shown that when such a high degree of polishing is achieved, pattern adhesion is no longer obtained. Perhaps better techniques for polishing the BN can be developed, but at present, this limitation exists. For this reason, beryllia appears to be the preferred substrate above 30 GHz. Using this material, and the techniques of Section II, it should be possible to fabricate resonators with resonant frequencies as high as 50 GHz, where the line width may be as small as one-quarter of a mil or 6 microns.

Frequency limitations on resonant loss are also imposed by rf considerations. These would include such properties as the loss characteristics (Q) and power handling capability.

Ideally, resonant loss provides no loss in the tube's operating band and sufficient loss at the BWO frequency to suppress oscillations. Usually, however, some loss "spills over" into the operating band if enough loss is provided at the BWO frequency for stability. Spillover becomes a problem as one goes higher in frequency, partly because of the limitations on the achievable sharpness of the loss frequency characteristics and partly because as one goes higher in frequency, typically the separation between the upper band edge and the oscillation frequency becomes smaller and smaller. Thus, for example,

E-F band tubes have been fabricated with resonant loss which introduced no in-band loss. G-H-I band tubes (specifically, 5 - 10 GHz) have been fabricated with resonant loss introducing 2 dB of loss at the upper band edge. Resonators for an I-J band tube (specifically, 8 - 18.5 GHz) have been fabricated and have been shown to introduce about 10 dB of loss at the upper band edge. In the first case (E-F band), the π -frequency was 7 GHz, and in the second case (G-H-I band), it was 14 GHz; in the last one, it was 21 GHz. Clearly, the separation between upper band edge and BWO frequency is becoming smaller and smaller. The resonant loss characteristics, however, appear to be the same for any resonant frequency in the range from 2 to 18 GHz. That is, the ratio of the loss bandwidth, Δf , at a particular value of loss (say, 20 dB) to the resonant frequency is constant for any resonator pattern. This ratio ($\Delta f/f$) can be considered a resonator's Q, and thus, is equivalent to saying that the Q of these resonators is constant with frequency. During this program, several experiments were conducted to determine if the Q could be increased. These experiments included using thicker gold layers (up to five skin depths thick), different bulk materials (silver and copper), and smoother substrates. None of these increased the observable Q.

It may still be possible to use resonant loss in its current form in I-J band tubes, even though spillover at these frequencies appears to be large. Several alternatives suggest themselves. The first would be to design the tube to operate over a lower range of γ_a . This would increase the separation between the upper band edge and the oscillation frequencies. It may be necessary to resort to dispersion control techniques in order to accomplish this. Another alternative would be to use resonant loss over just the part of the output circuit. Clearly, the loss would have to be placed as far from the tube's output as possible in order to minimize its deleterious effects on efficiency. Also, the loss-free section would have to be short enough in order to be stable at the proposed operating current.

V. ACHIEVABLE PEAK RF POWER

A. PEAK POWER LIMITS

The achievable peak output power of octave bandwidth, PPM focused helix TWTs is limited by several frequency dependent factors as shown in Figure 8. These curves are taken from Reference 2. Clearly, the existence of backward wave oscillations is the fundamental power limiting factor. The most commonly employed BWO suppression technique used in high power helix TWTs today is a small pitch step located near the center of the tube's output section. Its magnitude is usually between 6% and 7%. The curve labeled "conventional design" shows the power levels achievable using this technique based on actual tube data. In 1973, Raytheon discovered a method for suppressing BWO which increased the achievable peak power levels by about a factor of five over conventional designs (Reference 3). The technique takes advantage of the loss provided by interaction between the fast space charge wave on the beam and the backward wave space harmonic to suppress backward wave interaction. The curve of Figure 8 for this technique is based on experimental Raytheon data (Reference 2).

The results of the measurements performed on resonant loss during this program indicate that if it is used to suppress BWO, there is no longer a limit on achievable peak power due to BWO. This conclusion is based on measurements showing that resonant loss provides high loss densities, between 2 and 3 dB per turn per support rod. With such loss densities, it is easy to introduce several hundred decibels of total loss at the suspected BWO frequency if three support rods are used. If more loss is needed, additional support rods with resonant loss deposited on them can be used. Figure 9 shows the "revised" peak output power limits for helix TWTs if resonant loss is used to suppress BWO. Thus the peak output power of helix TWTs is no longer limited by BWO if resonant loss is used.

It may be possible, however, that resonant loss shifts the peak power breakdown limit curve of Figure 9 to the left; i.e., the achievable peak output power may be limited by rf breakdown, rather than PPM focusing with

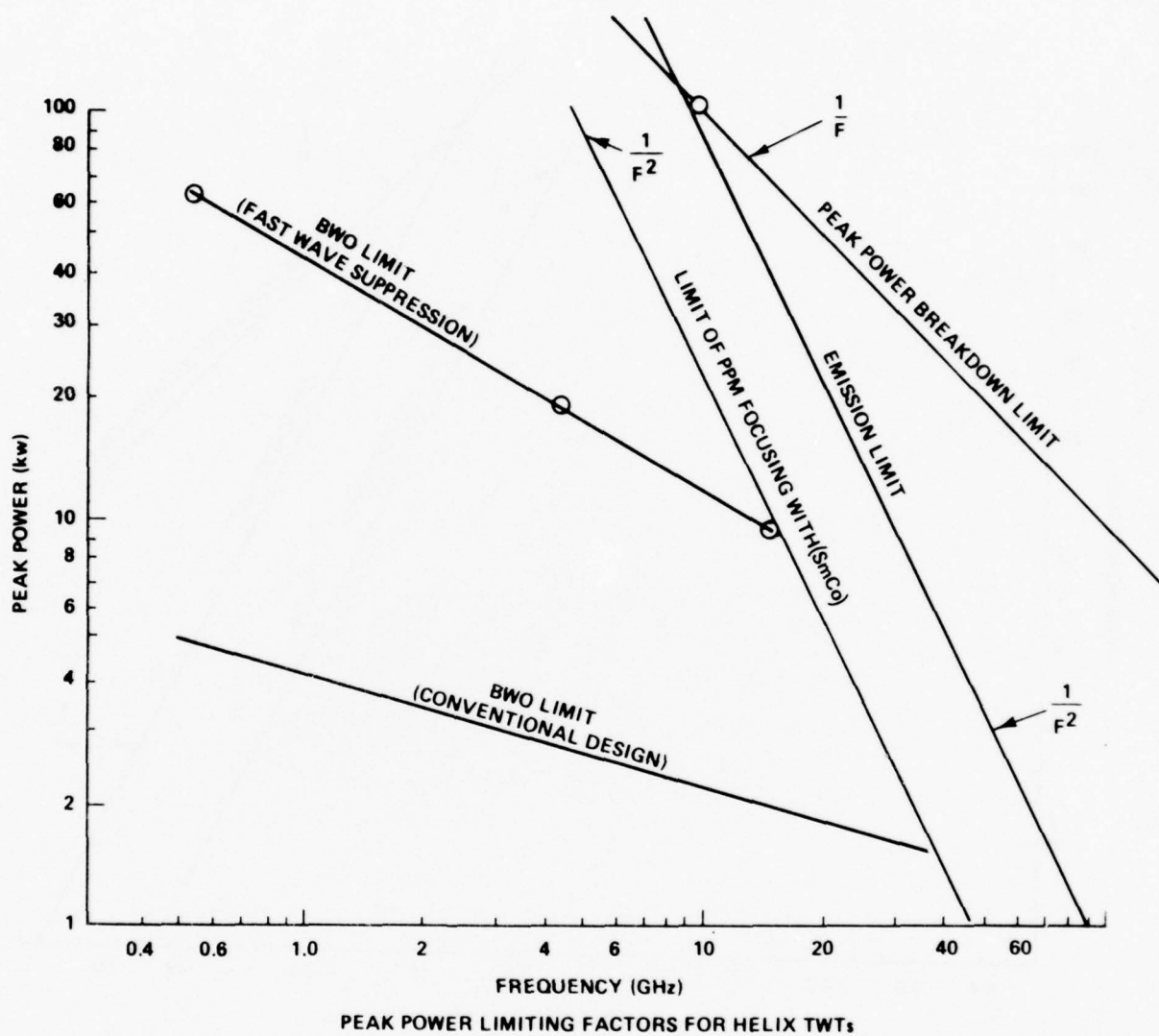


Figure 8. Peak Output Power Limits for Helix TWTs in 1974

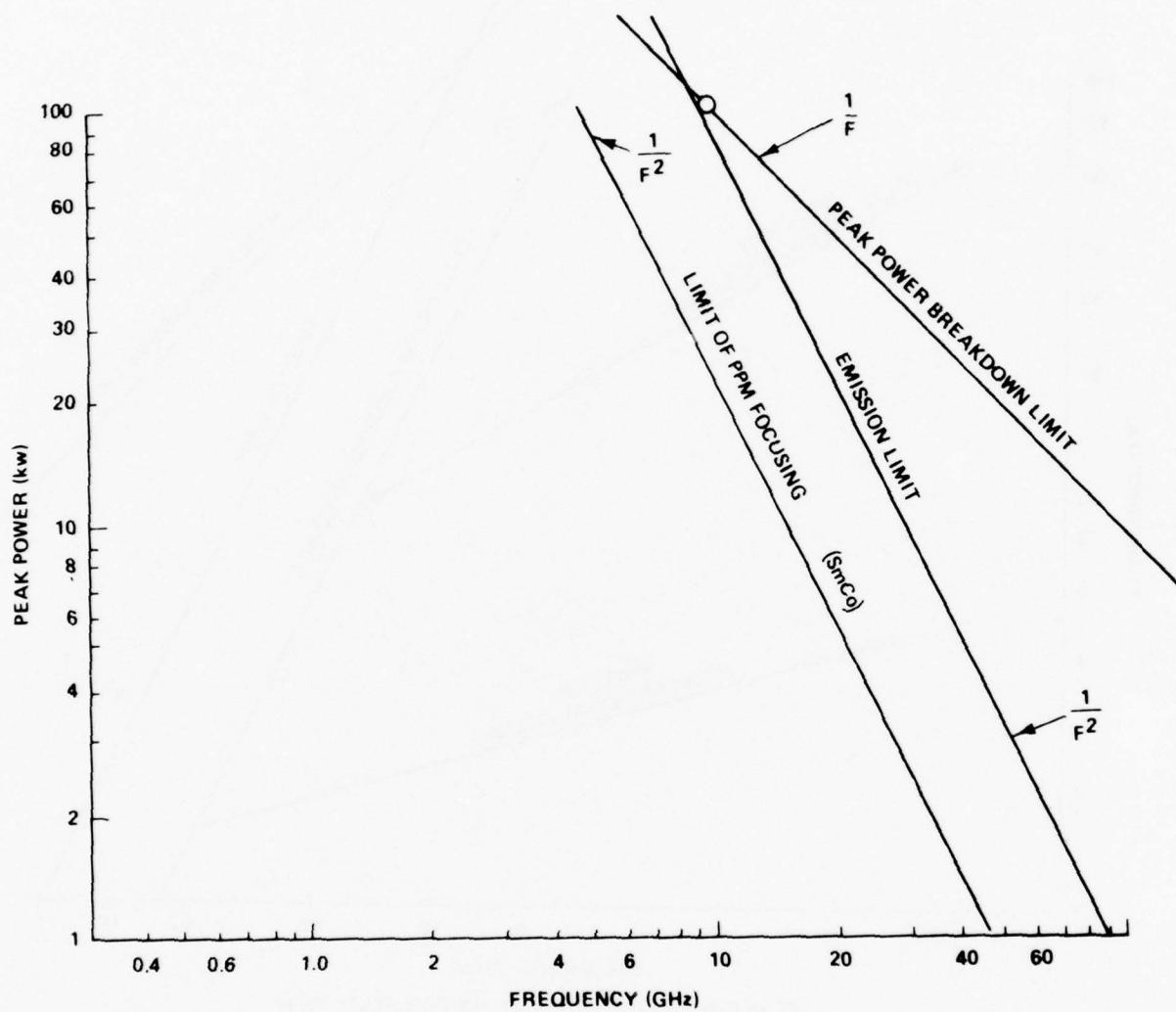


Figure 9. Peak Output Power Limits Other Than BWO for Helix TWTs in 1976

samarium cobalt. Later in this section, data will be presented on a tube which was built to demonstrate high peak power which exhibited rf arcing. For this and higher power tubes, it may be necessary to place resonant loss far from the output of the tube or further away from the helix (on the support rod). The latter would require that larger barrel to helix diameter ratios be used. Another possibility would be to sputter boron nitride or another insulator over the resonators.

B. HIGH PEAK POWER TWT

One of the goals of this program was to build an octave bandwidth helix TWT which would demonstrate high peak power, specifically, 10 kW from 3.5 to 7.0 GHz, utilizing only resonant loss for BWO stability.

One tube was built and tested during the latter part of the program. The tube's slow wave circuit is shown in Figure 10. The helix is made of 0.010" by 0.075" tungsten tape and is supported by three 0.030" thick pyrolytic boron nitride support rods in a 0.360" diameter barrel. The tube was built in three sections, each separated from the other by a sever, in order to achieve a minimum small signal gain of 50 dB. The helix pitch was 0.177" (5.65 TPI) throughout the length of the tube. Resonant loss was placed on all three support rods along the entire length of each section.

In order to determine the amount of loss required at the BWO frequency for stability, start current calculations were made for each section. The results are shown in Figure 11. The calculations were done assuming a helix pitch of 0.169", rather than the actual 0.177". This was done to simulate the reduction of a circuit's forward wave velocity due to resonant loss. The exact reduction cannot be predicted, and so it was assumed to be 4.5% based on earlier measurements. It will be shown later that the reduction was greater than this. The results of Figure 11 show that a minimum loss density of 4 dB per inch for the input and center sections and 8 dB per inch for the output section was required for stability at the proposed beam current of 4.1 A. Eight decibels per inch for a pitch of 0.177" is equivalent to 0.47 dB per turn per rod if three rods are used. When these calculations were made, it

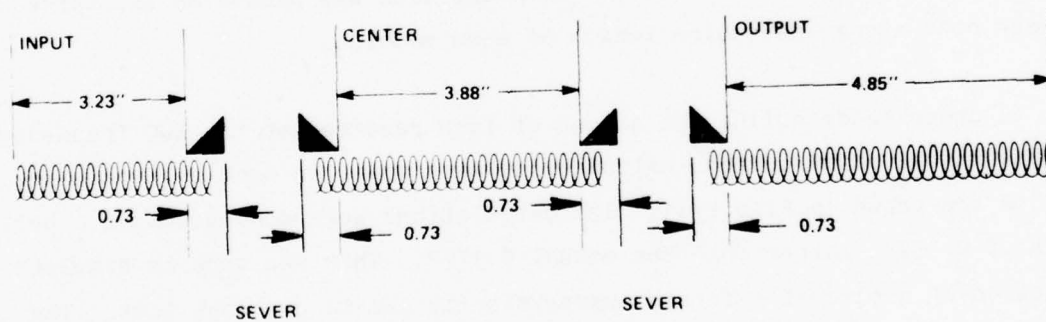
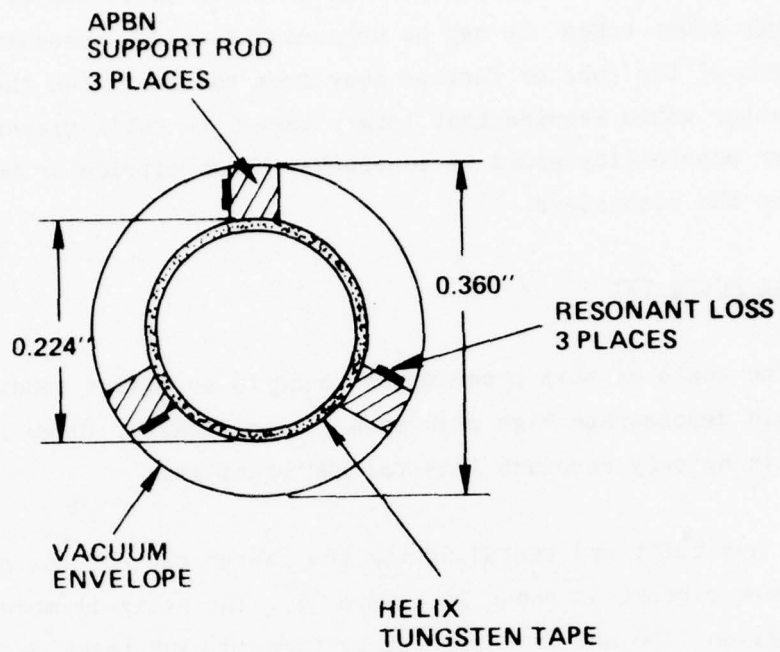


Figure 10. Ten Kilowatt TWT Slow Wave Circuit

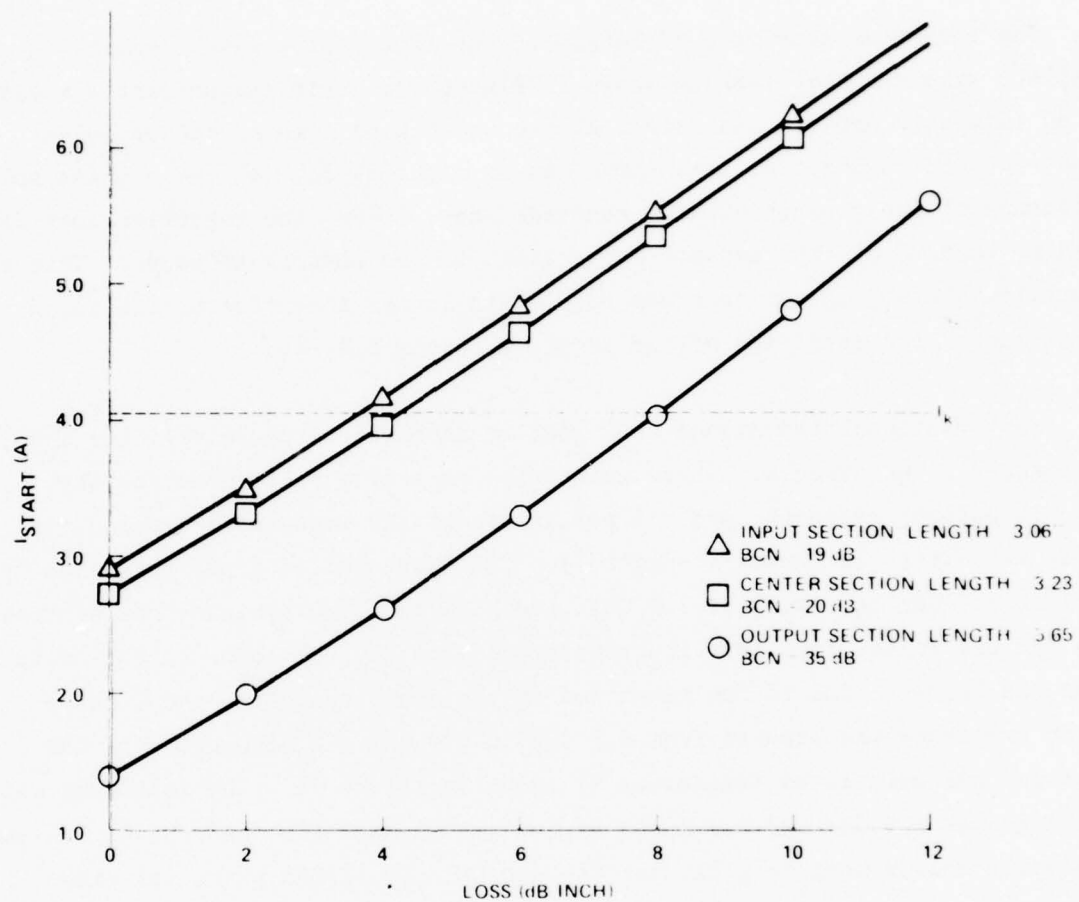


Figure 11. BWO Start Current Calculations

was not known if this loss density could be achieved. Thus, to be on the safe side, the resonators were not centered on the rod between the helix and barrel but rather, placed closer to the helix. This increases the coupling between the helix and the resonator and results in higher loss at the BWO frequency.

The insertion loss of a 6" length of the tube's slow wave circuit complete with resonant loss is shown in Figure 12. This measurement was made on an automatic network analyzer. At the upper band edge of the proposed band, 3.5 to 7.0 GHz, the insertion loss is high, 14 dB. At the π phase shift frequency of the circuit without resonant loss, 8 GHz, the insertion loss is greater than 70 dB, the dynamic range limit of the network analyzer. This is equivalent to 0.7 dB per turn per rod. This is far in excess of the value required for the stability of the output section, 0.47 dB.

Perturbational techniques were used to measure the phase velocity and impedance of the circuit. These quantities were also calculated for the circuit without resonant loss. A comparison of the measured and calculated phase velocities is shown in Figure 13. The phase velocity was decreased by 7.2% at 3.5 GHz and 14.4% at 7.0 GHz. Such large reductions are not typical and are due to the fact that the resonators were placed closer to the helix than the barrel. Due to the reduction of the phase velocity, the π phase shift frequency was lowered from 8.0 GHz to 6.9 GHz. A comparison of the measured and calculated impedances is shown in Figure 14. The impedance was unchanged at 3.5 GHz and decreased by 29% at 7.0 GHz. The uncertainty in the impedance measurement is $\pm 8\%$, and the uncertainty in the phase velocity measurement is $\pm 0.5\%$.

Using measured phase velocity, impedance, and loss data, the small signal gain of the tube was calculated and is shown in Figure 15. The proposed operating band, 3.5 to 7.0 GHz, has been shifted downwards in frequency. At a beam voltage, 20 kV, and beam current, 3.50 A, the small signal response is flat over the band from 3.0 to 6.0 GHz, and is almost 50 dB at this band's edges. This shift of operating band is due to the decrease of the phase velocity by the resonant loss.

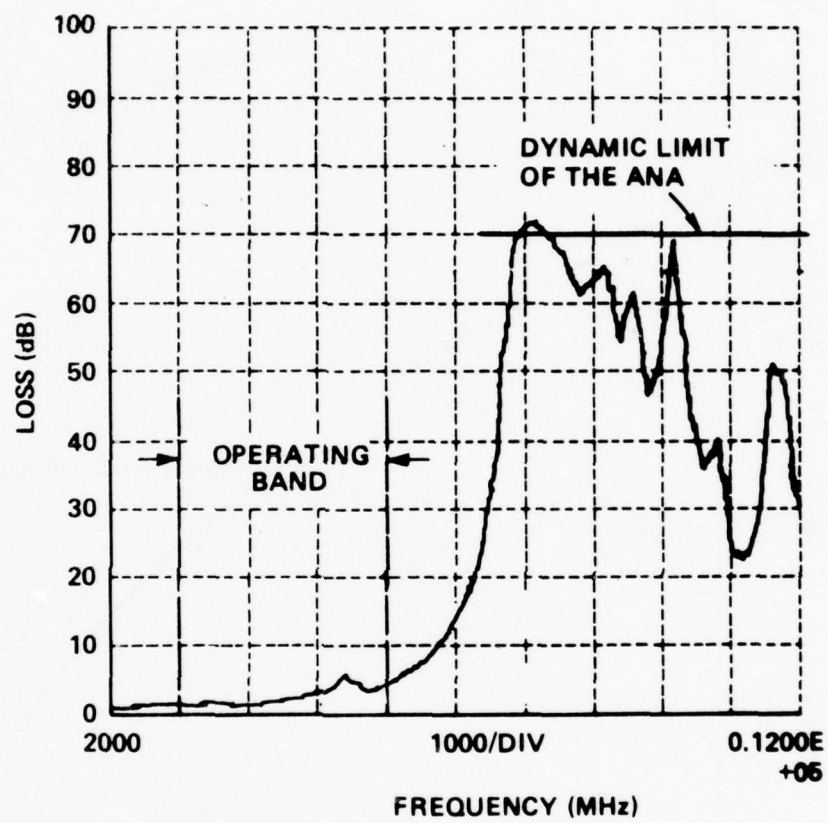


Figure 12. Measured Resonant Loss Characteristic

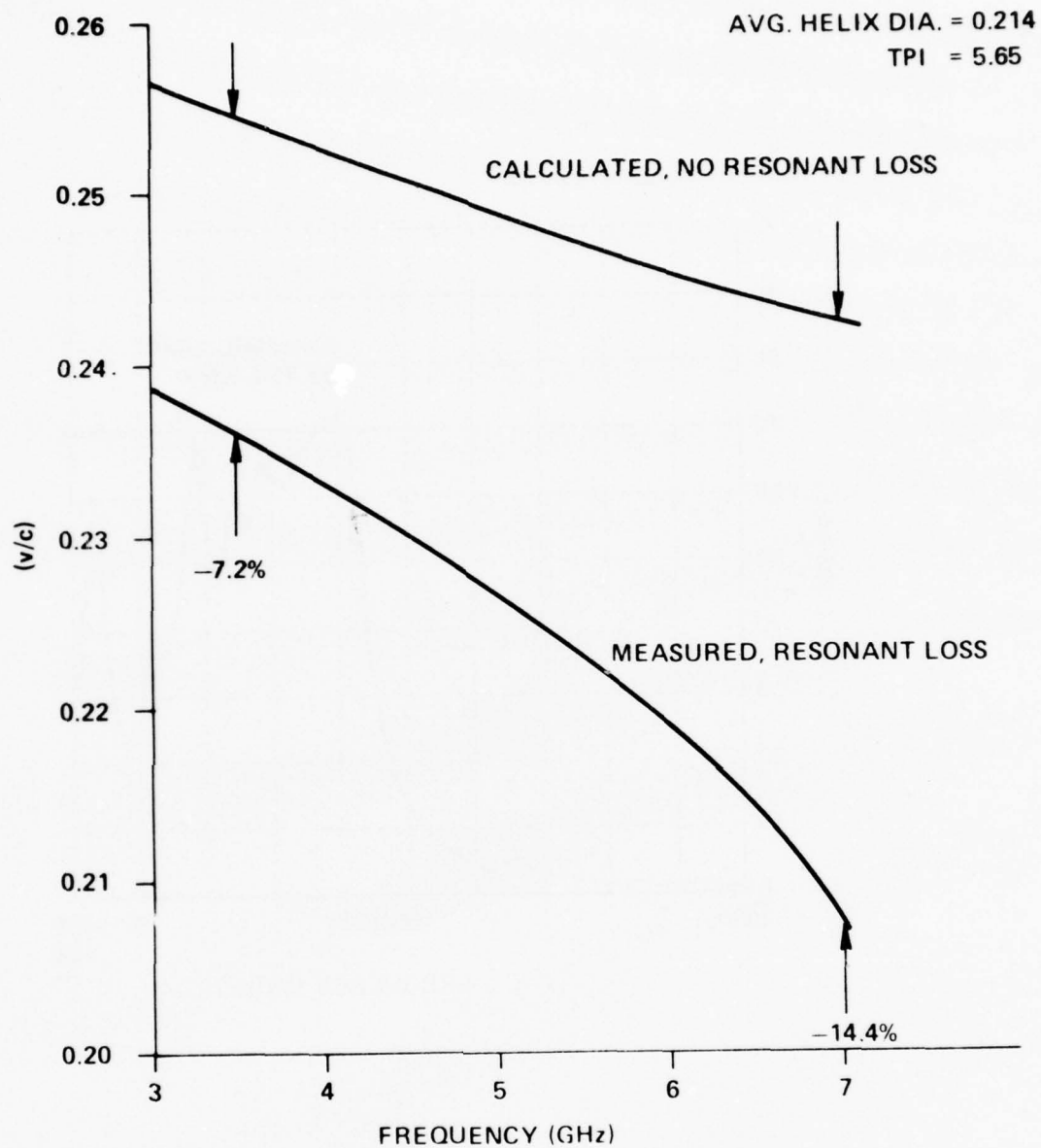


Figure 13. Comparison of Calculated (Without Resonant Loss) and Measured (With Resonant Loss) Phase Velocity

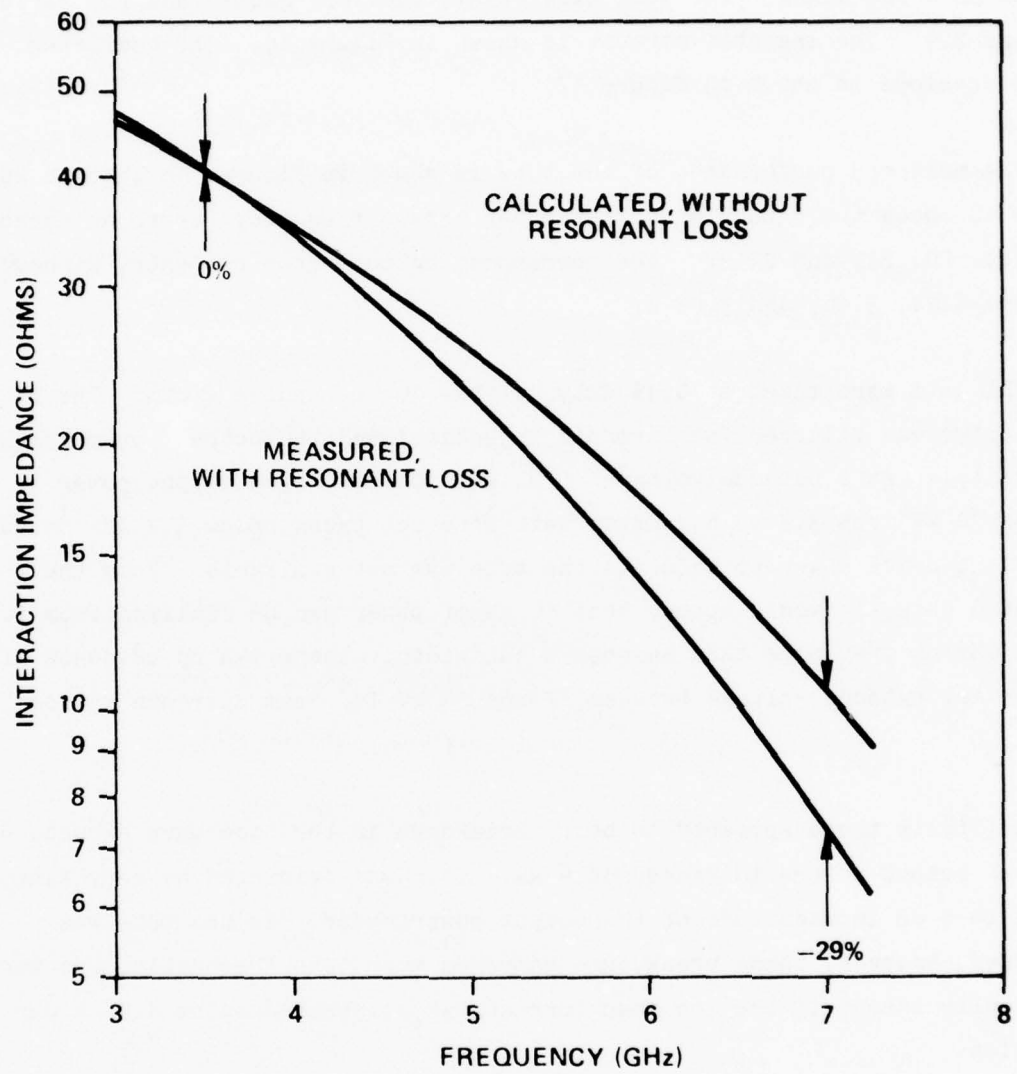


Figure 14. Comparison of Calculated (Without Resonant Loss) and Measured (With Resonant Loss) Interaction Impedance

The electron gun used on the tube had both shadow and control grids for beam control. Designed to operate at a microperveance of 1.3, the beam diameter was approximately 0.080". The beam was focused using samarium cobalt magnets in a PPM stack. The peak axial field was 1850 gauss, and the ratio λ_p/L was 2.9. The magnetic circuit is shown in Figure 16. The completed vacuum envelope is shown in Figure 17.

The measured performance of the tube is shown in Figures 18 through 20. Figure 18 shows the saturated output power versus frequency for three cathode voltages, 20, 21, and 22 kV. The corresponding collector currents, without rf, were 3.21, 3.16, and 3.03 A.

All data were taken at 0.1% duty, with a 10 μ sec pulse width. The rf input drive was filtered (no harmonic injection) and the output power is pure fundamental. At a cathode voltage of 22 kV, the saturated output power exceeds 10 kW from 3.2 to 6.2 GHz. Data were not taken below 3.2 GHz because sufficient drive power to saturate the tube was not available. From the saturated data, it would appear that 10 kW of power can be realized from 3.0 to 6.2 GHz or over more than an octave bandwidth. There was no evidence of BWO for any cathode voltage between 17 and 24 kV for beam currents up to 3.5 A.

Initially there appeared to be rf breakdown in the slow wave structure for peak output powers in excess of 9 kw. This was evidenced by very fast dips 3 to 4 dB in magnitude of the output power meter. As the tube was processed, however, these breakdowns happened much less frequently, and were essentially absent if the ion pump current was maintained below 1.5 μ A during operation.

The saturated gain data corresponding to the saturated power data of Figure 18 are shown in Figure 19. Figure 20 shows a swept small signal gain curve at a cathode voltage of 21 kV and a beam current (without rf) of 2.46 A. The small signal gain data were taken at this reduced current due to deterioration of the beam transmission. This deterioration occurred after about 50 hours of tube on-time, making the beam transmission at a cathode voltage of

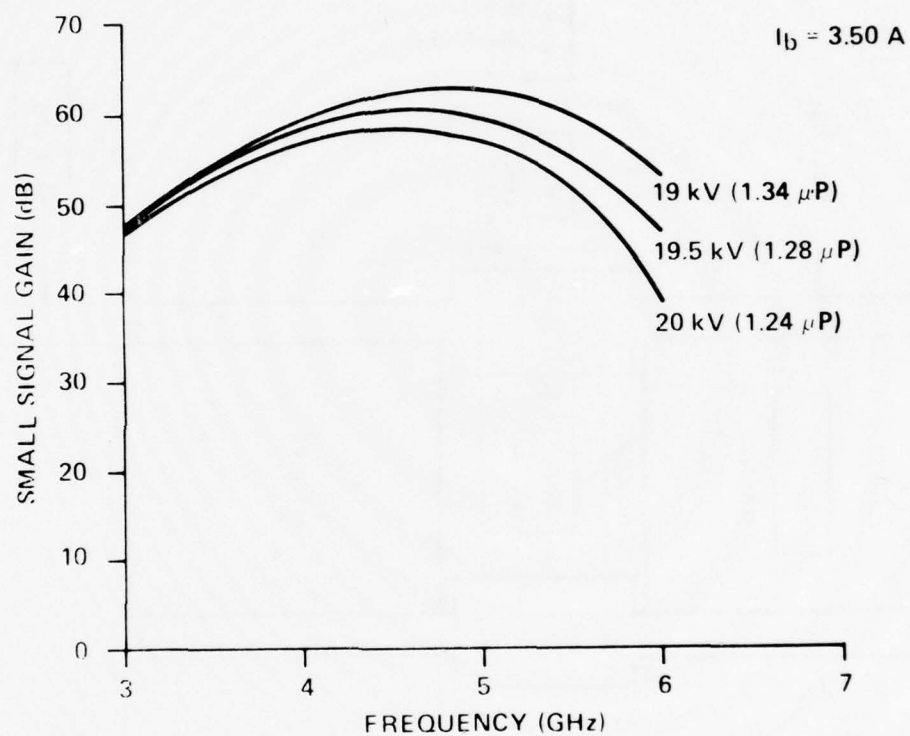


Figure 15. Calculated Small Signal Gain

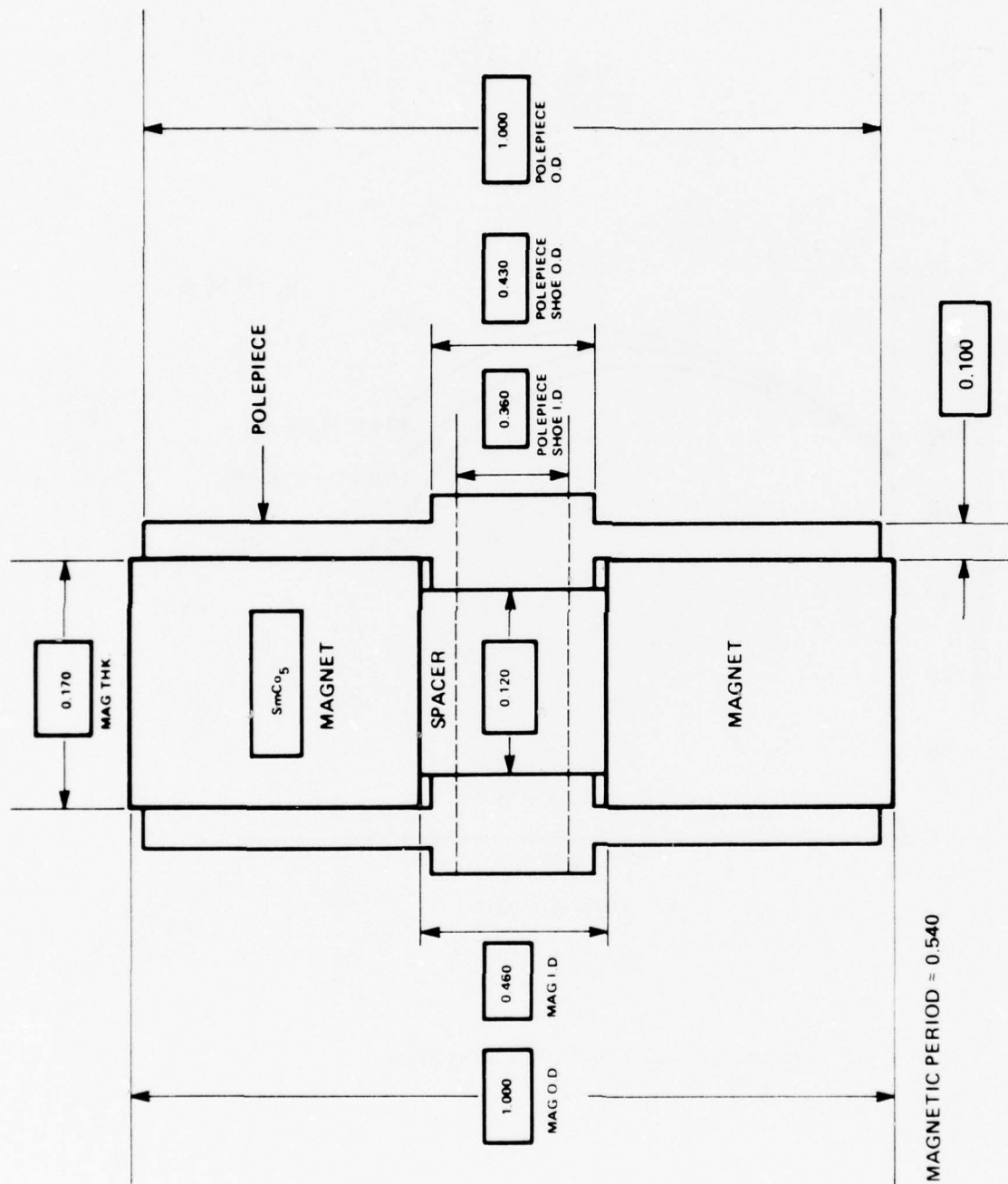


Figure 16. Magnetic Circuit

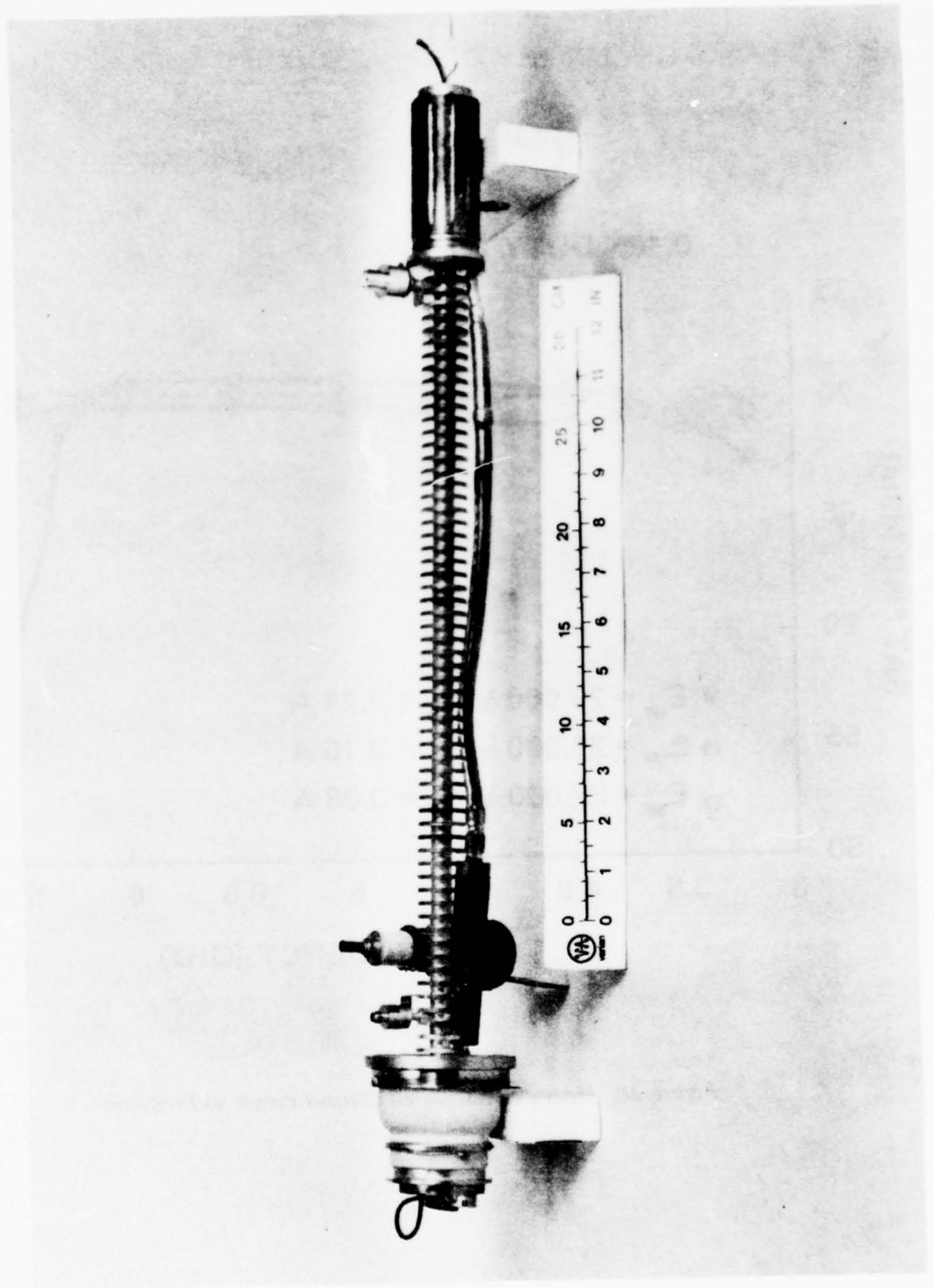


Figure 17. Ten Kilowatt TWT

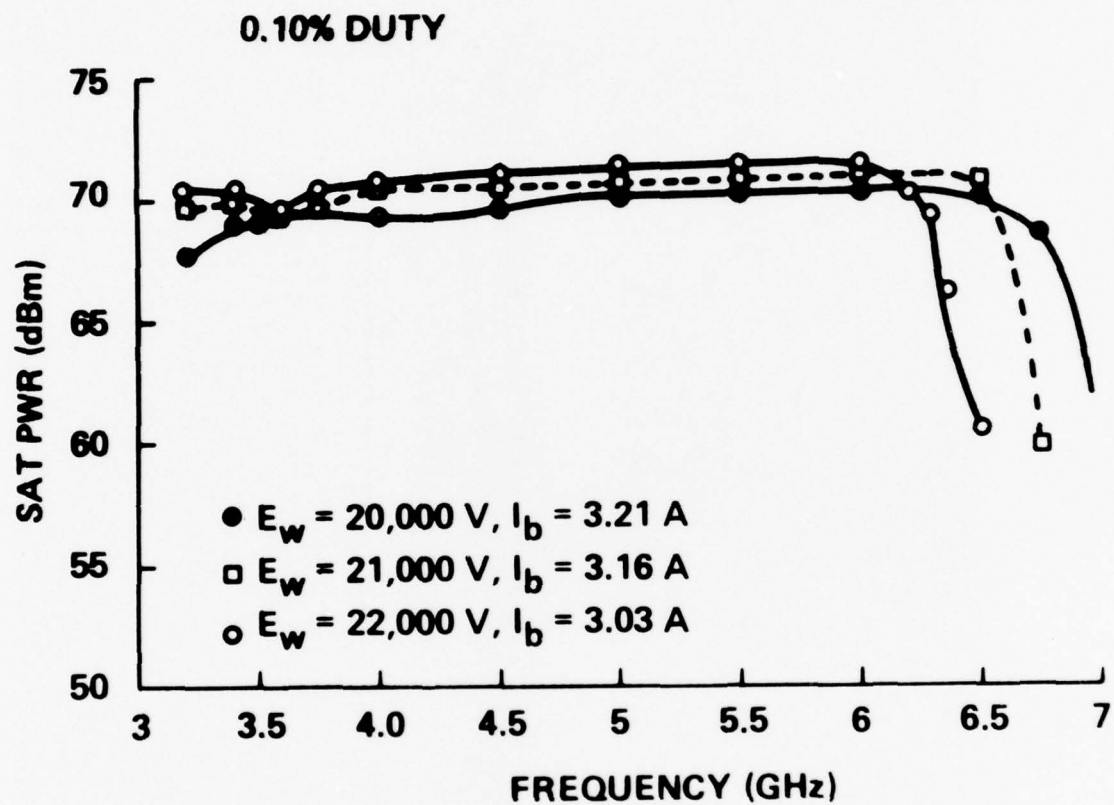


Figure 18. Measured Saturated Output Power vs Frequency

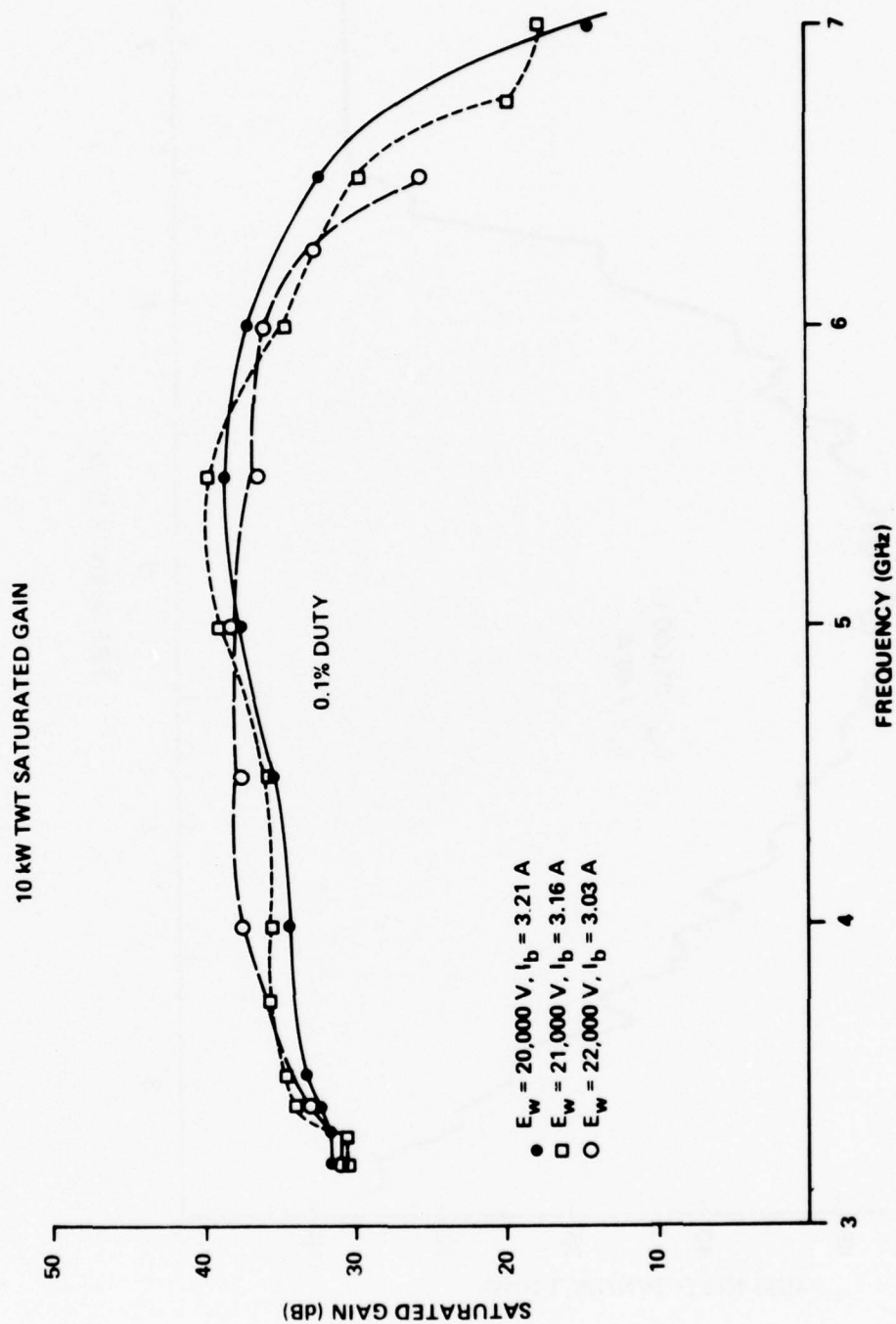


Figure 19. Measured Saturated Gain vs Frequency

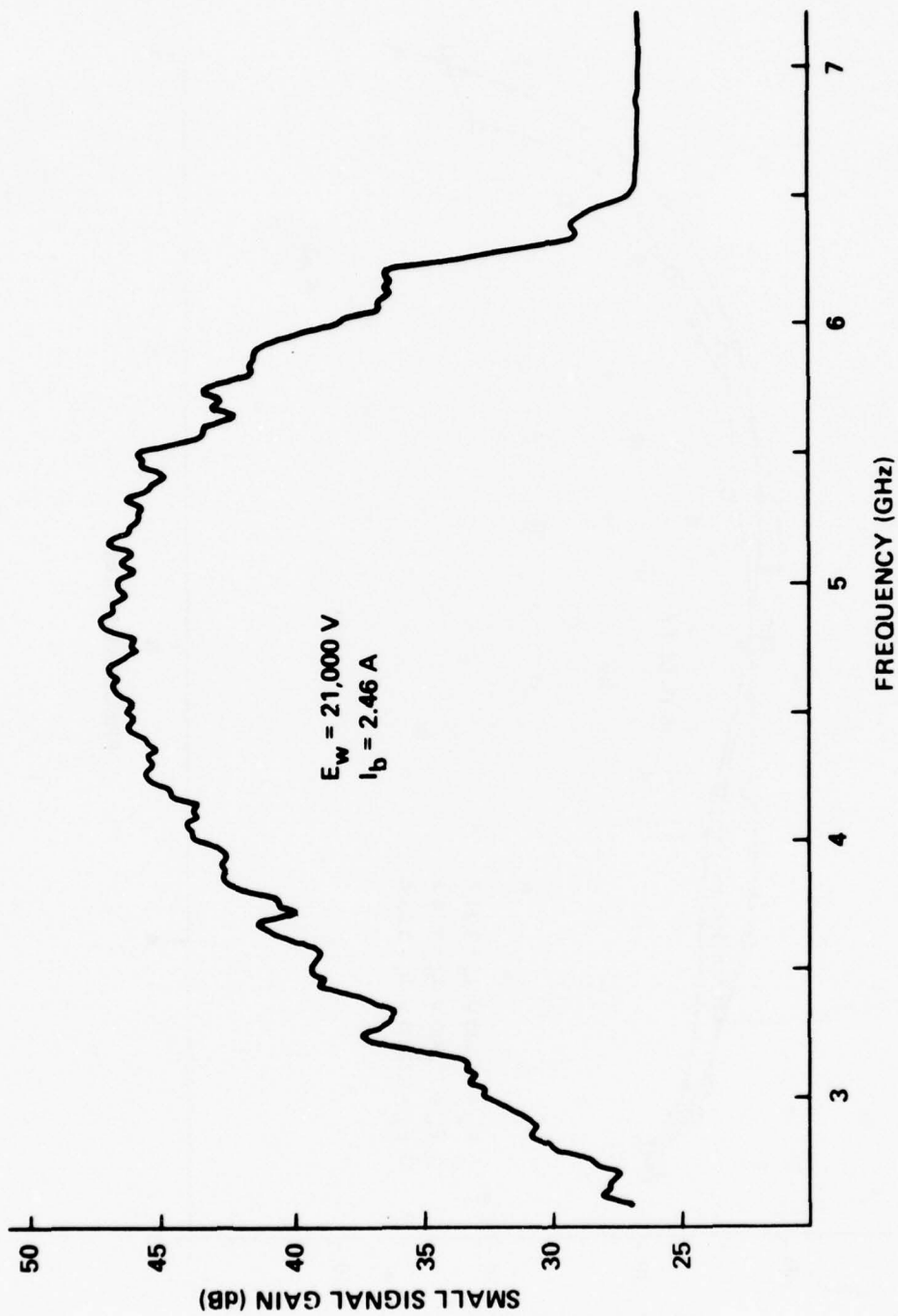


Figure 20. Measured Small Signal Gain vs Frequency

20 kV about 80% or less rather than the 93% or better value it had earlier. At the same time the tube began to backward wave oscillate very slightly (worst case level 20 dB below carrier) near 6.9 GHz, the π phase shift frequency. Initially the oscillation could be eliminated by placing small shunts on the PPM stack near the input window. After about ten more hours of operation, however, it could not be eliminated in this manner. After about 100 hours of total on-time, the tube was disassembled for analysis. The support rods of the output section were randomly coated with dark deposits in the areas between the resonator patterns and the helix and barrel. It would seem that these deposits were tungsten evaporated from the helix when the rf breakdown occurred. All of the resonators were still intact, even though portions of them appeared to have melted near the edges where the rf breakdown occurred. Each of the rods was individually placed in the 6" length of circuit and the insertion loss of this structure measured. The resonance was no longer present. It appears as if the patterns were shorted out by a thin layer of conductive material, most probably carbon and/or tungsten. The barrel of the output section was also coated with a dark, thick deposit. This may have been carbonized glue which deposited during the stuffing operation.

VI. COMPATIBLE DISTRIBUTED LOSS

There are at least four ways to incorporate both distributed and resonant loss into a helix TWT.

A. PYROLYTIC DEPOSITION

Probably the most common method of implementing distributed loss is to deposit a thin film of carbon by pyrolysis of a gaseous organic compound, preferably methane. However, this method cannot be used to deposit both resonant and distributed loss to the same rod. The pyrolytic carbon necessarily covers the entire rod, including the resonators and thereby "shorts" them out so that they no longer resonate.

No method could be devised to selectively coat a rod by pyrolysis which did not cover the resonators. However, it was possible to build a tube with resonant loss on two rods and distributed loss on the third which was stable. This asymmetric loss distribution has other consequences, however, and these are discussed in Section IX.

B. COLLOIDAL CARBON

The spraying of colloidal carbon onto support rods is probably the oldest technique for implementing distributed loss. Clearly this would be a method for applying both resonant and distributed loss to the same rod. Since colloidal carbon is usually sprayed onto the rod at room temperature, the resonators could be easily masked, say with glue, during the spraying so that the carbon did not short them out.

C. SPUTTERED FILMS

Thin, conducting films may be used to supply broadband rf loss. Because they are sputtered, it is easy to apply them selectively. They may be pure metals or compounds. During the course of the program molybdenum, titanium carbide, and tungsten carbide were tried as distributed loss materials.

Titanium carbide did not appear to adhere as well as the other two. An added disadvantage is that it cannot be hydrogen fired since titanium-hydride is formed and the loss changes or is simply lost. It appears that both molybdenum and tungsten carbide in two to three thousand angstrom thicknesses gives reasonable loss density values; e.g., 1 to 3 dB per inch.

D. LOW Q RESONANT LOSS

Low Q meander line resonant loss tuned to in-band frequencies can be used to provide distributed loss. If the bulk resonator material is thin enough, resonators provide loss which is about as frequency sensitive as pyrolytic carbon. For example, if molybdenum is used as the bulk material, this thickness is less than about 5000 Å. In thicker coatings, resonators will provide slightly selective loss. For molybdenum, this thickness is about 10,000 Å. If such resonators were tuned to the middle of the tube's operating band, they would tend to flatter the tube's small signal gain characteristic, clearly a desirable feature.

VII. IN-BAND EFFECTS OF RESONANT LOSS

Resonant loss decreases the phase velocity and impedance of a circuit. However, if the helix pitch is adjusted to compensate for the presence of resonant loss (so that the tube operates at the desired voltage), it appears that most of the impedance is recovered. Resonant loss also increases the dispersion of a circuit slightly.

The exact magnitude of the velocity reduction cannot be predicted theoretically, but typical values have been obtained from the measurements made on circuits before and during this program. For tubes operating between 2 and 18 GHz with a helix-resonator distance to average helix diameter ratio between 0.03 and 0.04, the velocity is decreased by 7% at the lower band edge frequency and by 10% at the upper band edge frequency. When resonant loss is added to a circuit, the impedance reduction does not appear to be as easily specified, partly because the uncertainty in its measurement is at least $\pm 8\%$. At the lower band edge, there appears to be no impedance reduction or even a slight increase. At the upper band edge, the reduction appears to lie between 15 and 30%. These values compare the impedance of the same circuit before and after resonant loss is added (same pitch). If the pitch is increased to speed up the circuit to the desired value, then the impedance reduction at the upper band edge is only about half this; i.e., 7% to 15%. This will be discussed more fully later in this section.

In order to estimate the effect of different helix to resonator spacings, several experiments were made. For each of the circuits measured, resonant loss with the characteristics of Figure 21 was employed. The circuit was from a tube operating from 5 to 10 GHz. The helix pitch was 0.0754", and the average helix diameter was 0.126". The standard barrel diameter is 0.208". Without resonant loss, the π phase shift frequency is 13.8 GHz. Figure 22 shows calculated and measured phase velocity data for two resonator to helix spacings. In the upper part of this figure, this spacing was 0.004". For this spacing, the helix-resonator spacing to average helix diameter ratio is 0.032, a typical value. The calculated and measured phase velocity curves for the circuit without resonant loss agree very well. When resonant loss was

added between each turn on all three support rods, the velocity was decreased by 7.6% at 5 GHz and by 10.6% at 10 GHz compared to the calculated values. The π phase shift frequency was lowered to 11.8 GHz because of the phase velocity reduction. In the lower part of this figure, the resonator to helix spacing was increased to 0.009", for a helix-resonator spacing to helix diameter ratio of 0.071. The barrel diameter had to be increased to 0.220" in order to do this. In this case the phase velocity was decreased by only 4.9% at 5 GHz and by 7.0% at 10 GHz compared to the calculated values. The π phase shift frequency here is 12.3 GHz.

It is interesting to note the shape of these velocity curves above 10 GHz, where the resonant loss is becoming very effective (cf. Figure 21). The phase velocity here is decreasing more rapidly (becoming even more dispersive) than in the operating band due to the high level of loss. Above 12 GHz the phase velocity cannot be measured because of the large amount of loss.

The interaction impedances corresponding to the phase velocity curves of Figure 22 are shown in Figure 23. For a 0.004" helix-resonator spacing, the impedance is decreased by 7.7% at 5 GHz and by 32.8% at 10 GHz. The impedance for a 0.009" spacing is actually higher by 3.4% at 5 GHz, while it is decreased by 18.5% at 10 GHz. The increased impedance at 5 GHz is a result of the inherent uncertainty of the measurement.

The decrease of the circuit phase velocity and impedance by resonant loss can be offset by increasing the helix pitch until the desired phase velocity is achieved. This was not done for the experimental H-I band circuit but the principal can be made apparent by additional calculations. Thus, if the pitch of the circuits without resonant loss is decreased until their mid band phase velocity is the same as the circuits with resonant loss, the impedance is also reduced. Figure 24 shows the measured phase velocity data of Figure 22 along with calculated values for pitches chosen so that the mid band velocities are nearly equal. The higher dispersion of the resonant loss circuits is still apparent. Figure 25 shows the corresponding interaction impedance data. At the high end of the band (10 GHz), where the impedance is affected most by

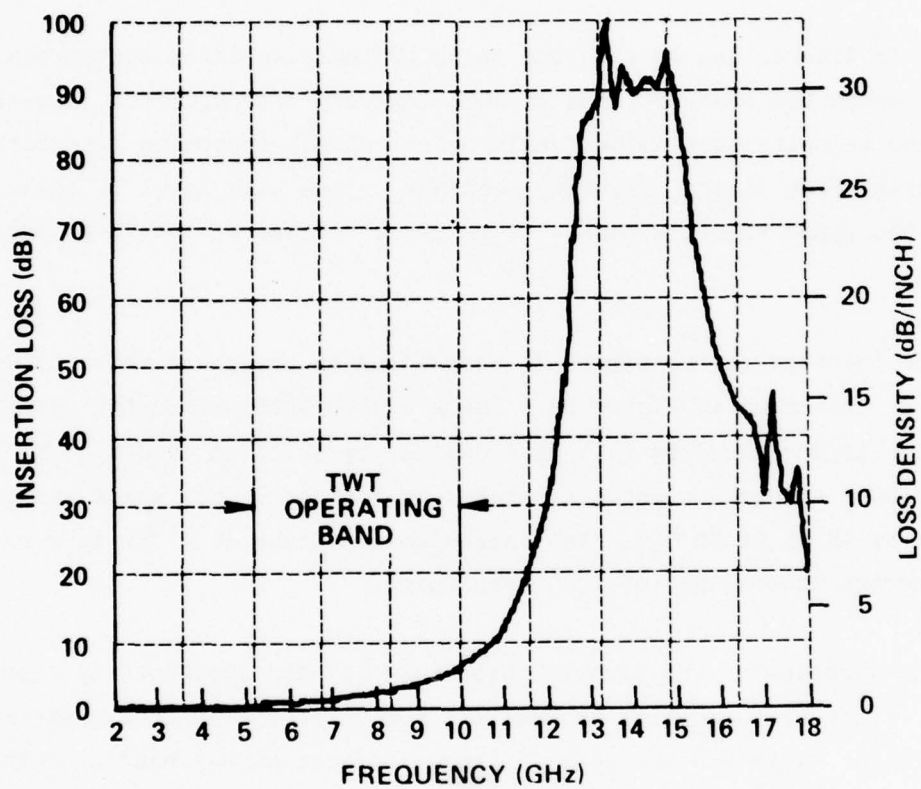


Figure 21. Measured Insertion Loss of Three Inch Length of G-H Band Circuit with Resonant Loss

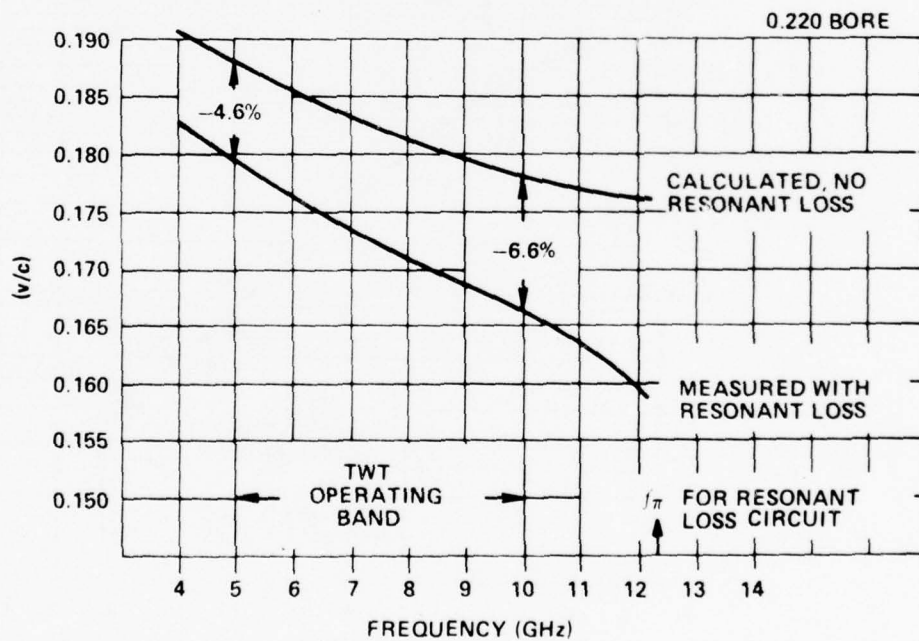
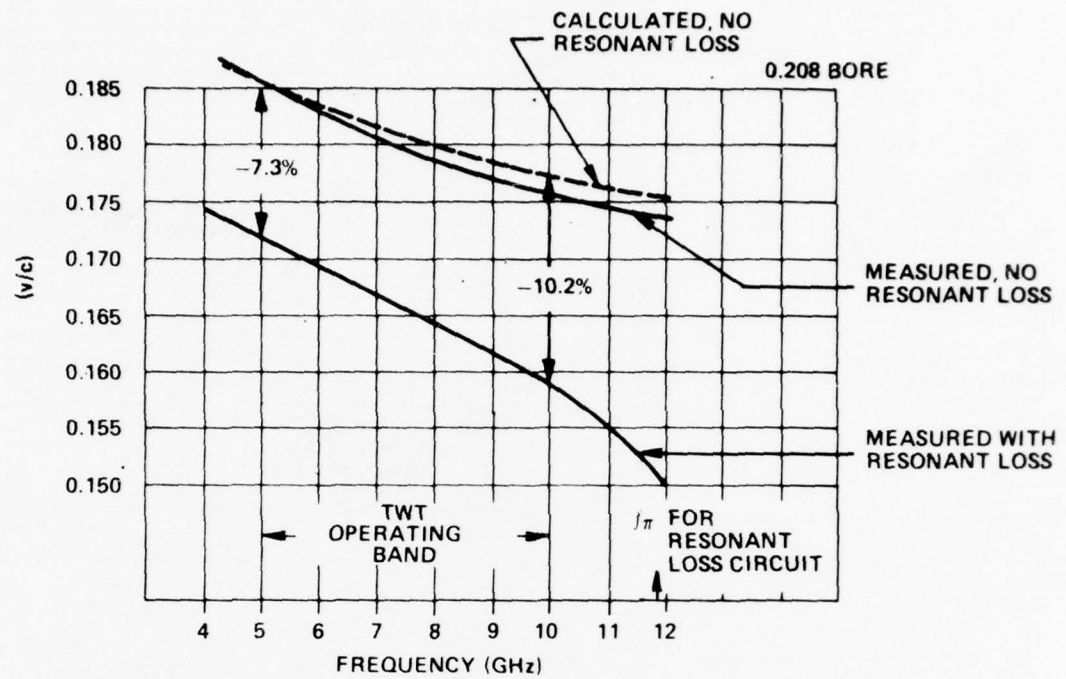


Figure 22. Phase Velocity vs Frequency for Circuits with and without Resonant Loss

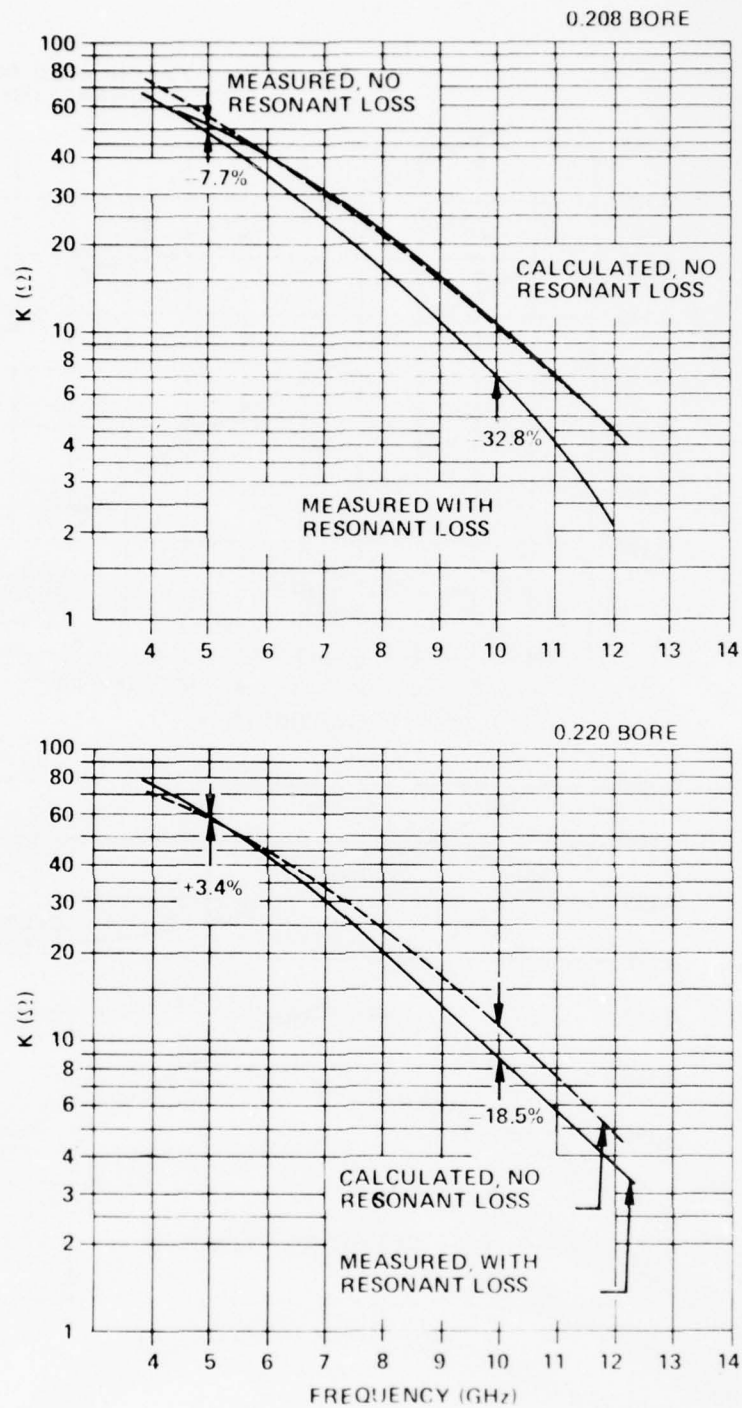


Figure 23. Impedance vs Frequency for Circuits with and without Resonant Loss

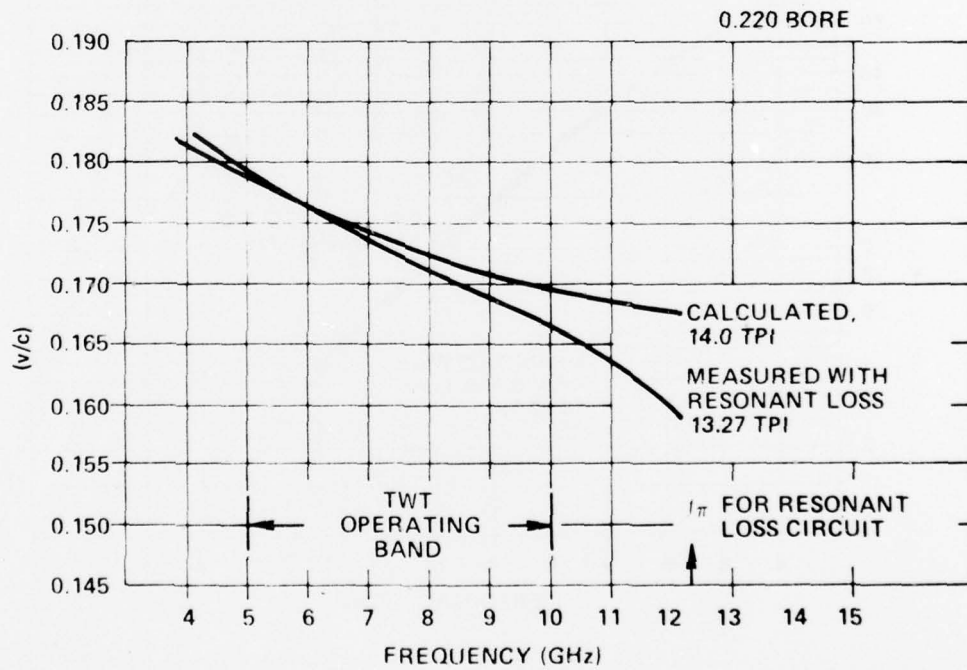
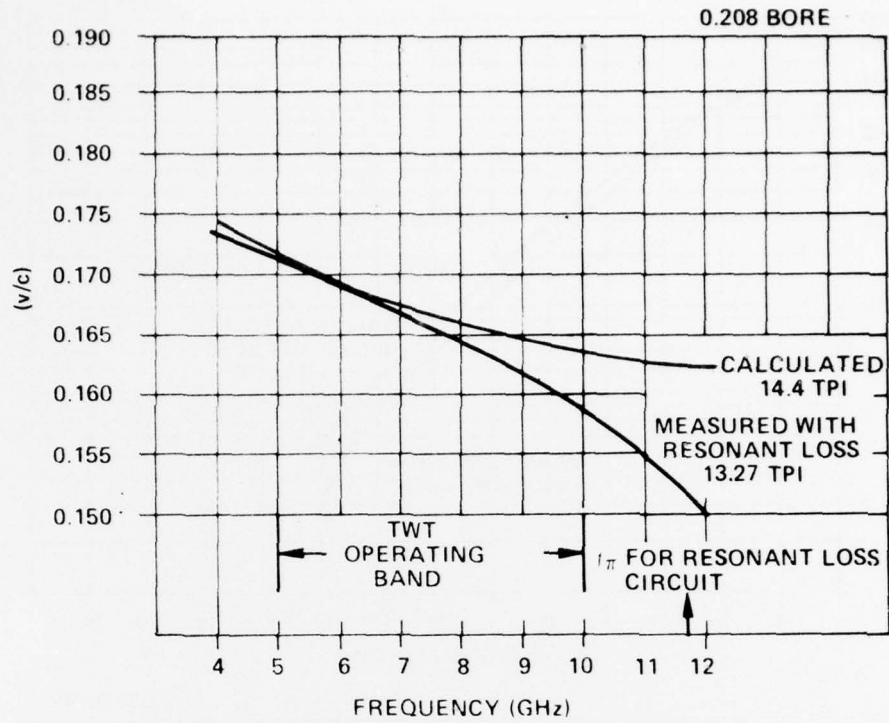


Figure 24. Phase Velocity vs Frequency for Circuits with and without Resonant Loss

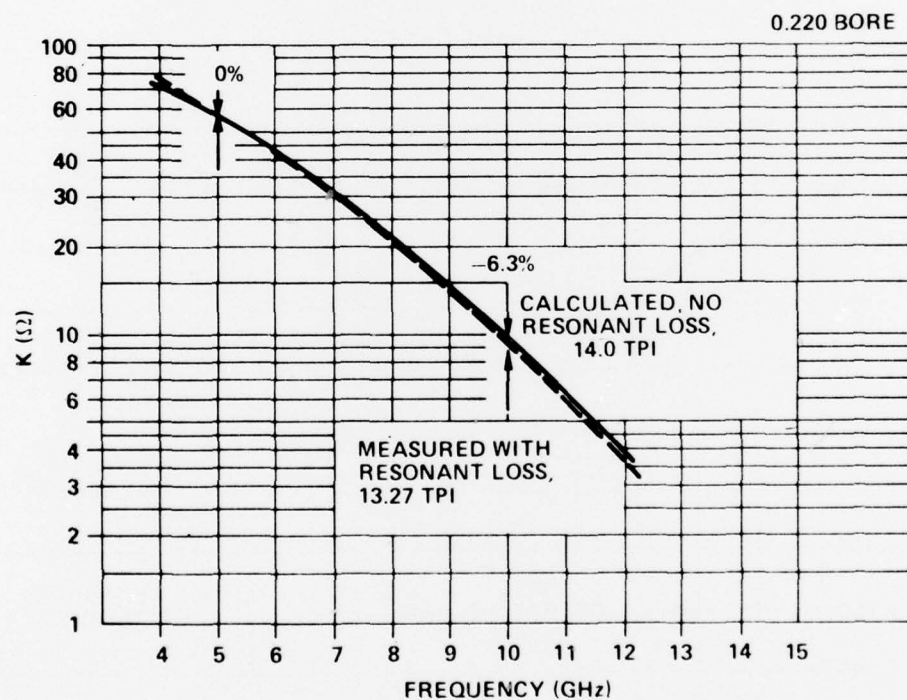
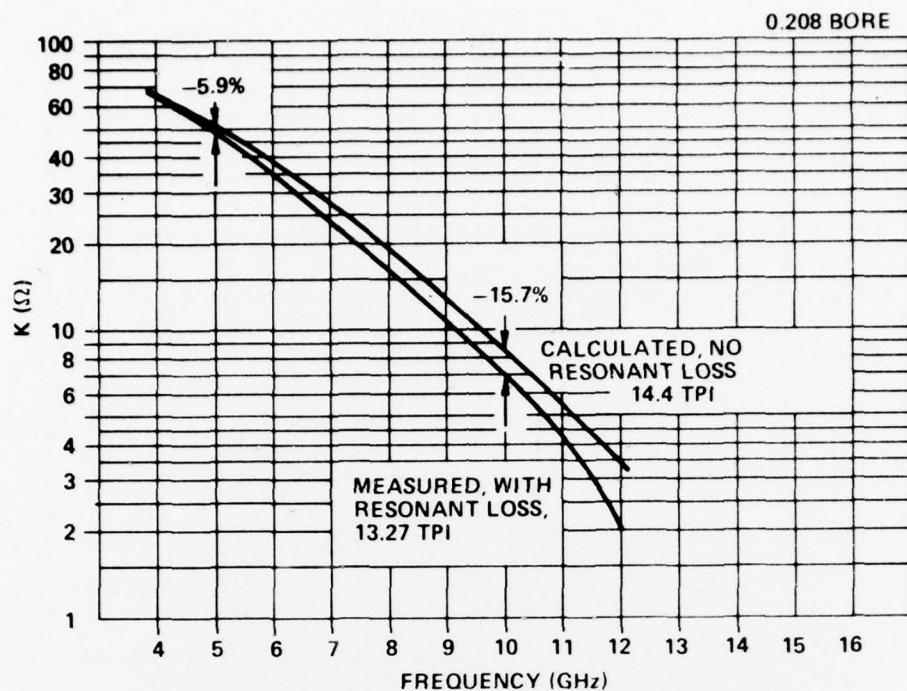


Figure 25. Impedance vs Frequency for Circuits with and without Resonant Loss

resonant loss, the pitch change has cut the percent impedance reduction by more than half. Thus, it would appear that resonant loss decreases the impedance of the scaled circuit (speeded up to account for resonant loss) by between 0 and 5% at the lower band edge and between 7 and 15% at the upper band edge. This conclusion is based on limited data, and, moreover, it must be remembered that the uncertainty in impedance measurements is $\pm 8\%$.

The above data and calculations suggest that the in-band effects of resonant loss are minimal, once the helix has been compensated for the phase velocity reduction. This assumes that resonant loss introduces little or no loss into the operating band. This appears to be the case for all but the highest frequency tubes (I-J band) explored. The next section discusses this topic in more detail.

VIII. FREQUENCY CHARACTERISTICS (Q)

Ideal resonant loss introduces no in-band loss while it provides sufficient loss at the BWO frequency to stop oscillations. In practice, whether resonant loss introduces in-band loss, depends on the separation between the upper operating band edge frequency and the BWO frequency. Thus, for tubes with peak or CW output powers up to 2 to 3 kW and operating with a maximum helix voltage of 10 kV, the current resonant loss scheme introduces no in-band loss for E-F band tubes because there is a large frequency separation between the upper band edge and the BWO frequency. For G-H band tubes with similar parameters, resonant loss introduces a maximum of 3 dB of loss at the upper band edge. For I-J band tubes in this range, the loss "spillover" can be as much as 10 dB. Figure 2 shows the insertion loss versus frequency for a 3.29" length of G-H-I band circuit with resonant loss. At the upper band edge (10 GHz) the resonant loss introduced 3 dB of loss over and above the loss of the circuit due solely to support rod and helix losses. Figure 26 shows the insertion loss versus frequency for a 1.5" length of I-J band circuit with resonant loss. The loss is relative to the insertion loss of the circuit without distributed or resonant loss. The upper band edge frequency is 18 GHz. The BWO frequency of the tube which uses a small pitch step and distributed loss for stability is 20.5 GHz. Resonant loss provides 43 dB of loss at 20.5 GHz, and introduces 9 dB at the 18 GHz.

The reason for the increase of spillover loss with increasing frequency for such tubes is that the separation between the upper band edge and BWO frequency becomes smaller with increasing frequency. This is due to the increase of the dielectric loading with frequency.

Higher peak or CW power tubes require the use of higher helix voltages, and this tends to decrease the separation between the upper band edge frequency and the BWO frequency. In some cases this decrease may even cause the BWO frequency to occur within the operating band; in which case, the only solution is to resort to lower γ_a operation. This was true of the 10 kW tube built during this program. From the measured phase velocity data, it can be seen that γ_a ranged from 0.695 to 1.522 over 3 to 6 GHz band. The helix

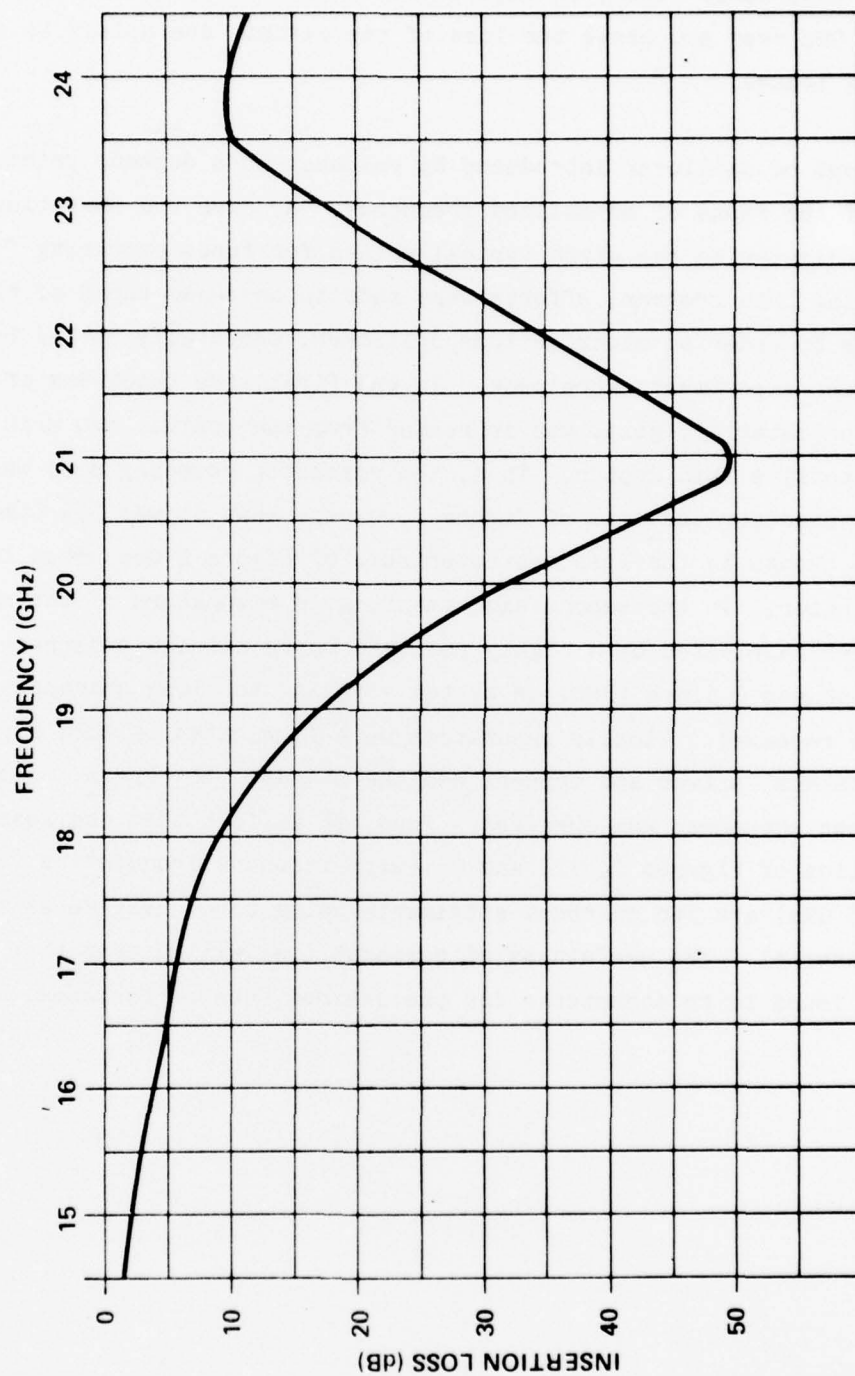


Figure 26. Insertion Loss vs Frequency of I-J Band Circuit with Resonant Loss

diameter was simply chosen small enough to move the BWO frequency far enough away from the upper band edge so that the resonant loss would not introduce excessive in-band loss. Thus, in Figure 12, the resonant loss introduced 3 dB of loss at 6 GHz over and above the loss of the circuit due solely to support rod and helix losses.

The amount of spillover introduced by resonant loss depends primarily on the choice of the range of normalized frequency, γ_a , over the operating band. The previous discussion has given typical values for tubes operating from 2 to 18 GHz. During this program, efforts were made to increase the Q of the resonant loss in order to minimize loss spillover, especially at I-J band. Three different experiments were made. In the first, the thickness of the bulk resonator material, gold, was increased from the nominal two skin depths (at 15 GHz) to five skin depths. Thus, the resonator geometry used was the same as that used for the data of Figure 2, except that it was 2.5 times thicker. No change in the loss characteristic of Figure 2 was noted for the thicker resonator. In the second experiment, gold resonators of the standard thickness were fabricated on a highly polished boron nitride substrate. The surface finish was 2 μ inch (RMS) or better. Again, the loss characteristic of Figure 2 was repeated. Finally resonators were fabricated of more highly conductive metals, silver and copper, and the standard thickness. Again, no change in loss sharpness was observed. Thus, it is felt that the loss characteristics of Figures 2, 12, and 26 (with resonant frequencies varying from 8 to 21 GHz) are the sharpest attainable using boron nitride as the substrate material. The usefulness of resonant loss will depend then on the range of γ_a found to be acceptable for the desired tube performance.

IX. ASYMMETRY EFFECTS

As mentioned in Section VI, asymmetric arrangements of resonant loss, i.e., depositing it on only one or two of the three support rods, have been used in tubes so that distributed loss can be applied to the remaining support rods. The effect of such arrangements is to introduce or exaggerate the stopband which normally occurs about the π phase shift frequency. Figure 2 shows the measured insertion loss of a G-H band circuit with resonant loss on all three support rods. Figures 27 and 28 show the same quantity for circuits with resonant loss on one and two support rods respectively. A stopband can be seen in each case, and in each case it is centered over the measured π phase shift frequency. The dashed line in each figure shows what the loss characteristic would be if the π frequency were not in the frequency range shown. Since the stopband increases the observed loss, such asymmetric arrangements would be acceptable.

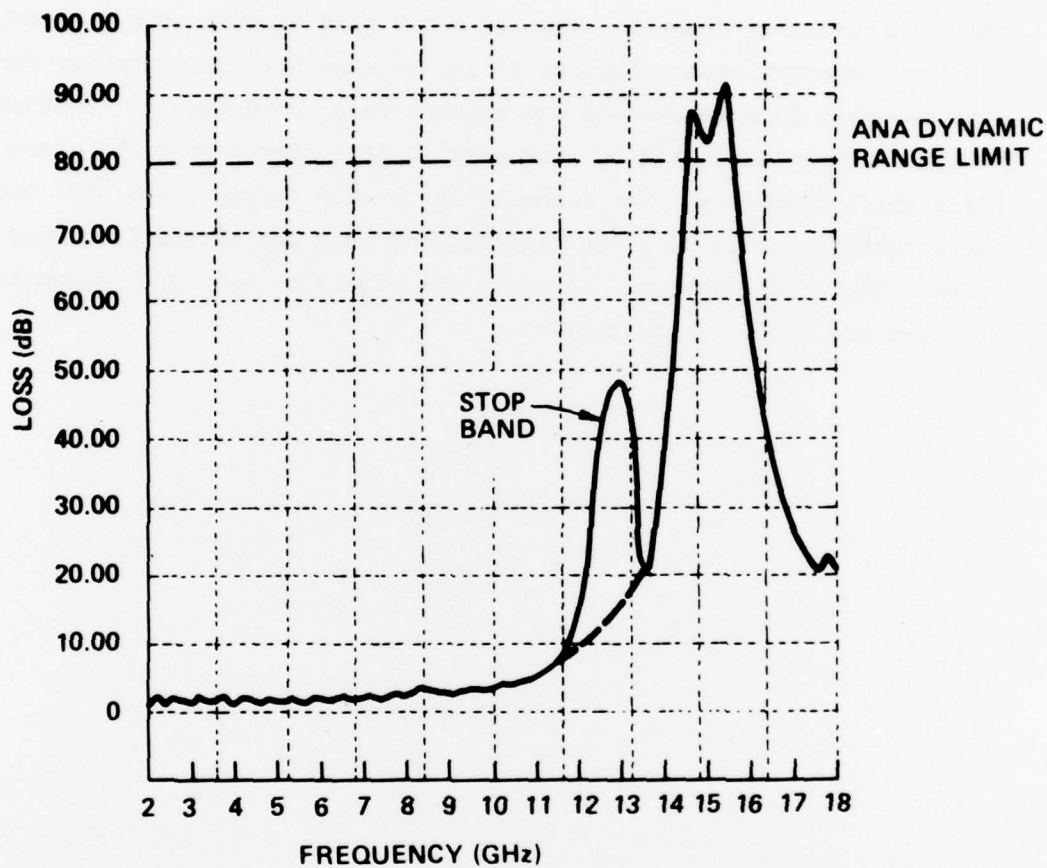


Figure 27. Measured Insertion Loss vs Frequency for G-H Band Circuit with One Resonant Loss Rod

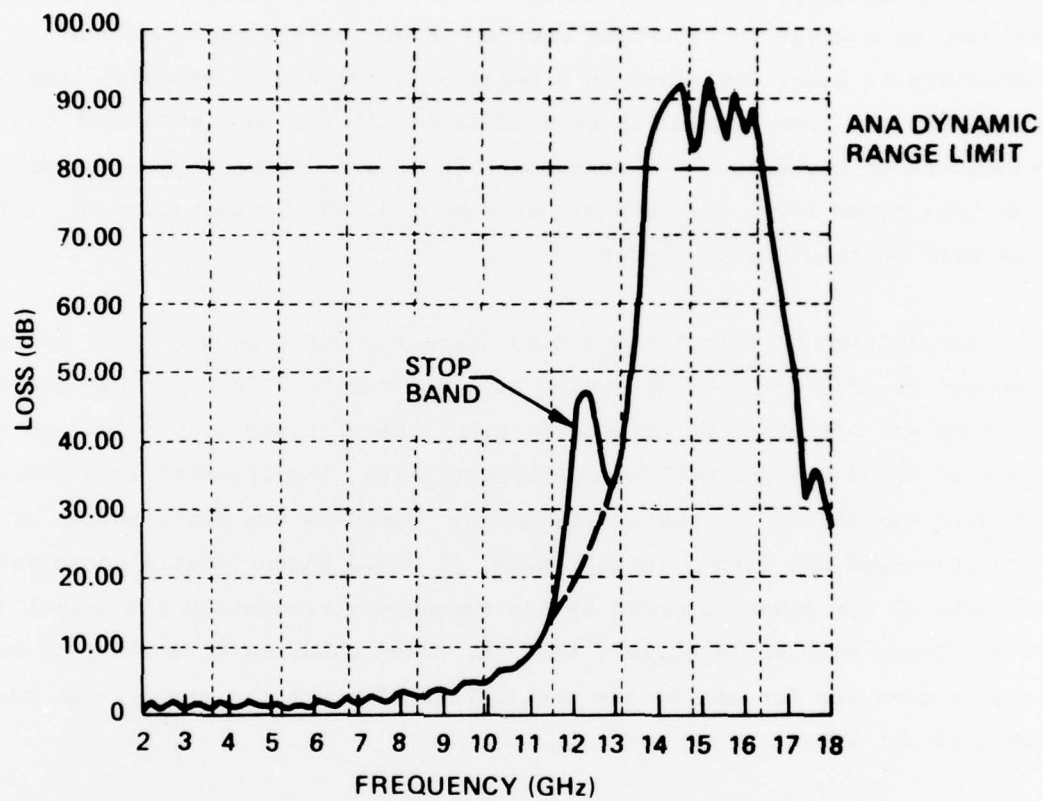


Figure 28. Insertion Loss vs Frequency for G-H Band Circuit with Two Resonant Loss Rods

X. POWER HANDLING CAPABILITY

Tests were conducted in order to determine the amount of rf power a resonator could absorb without being destroyed. A four inch length of helix circuit with resonators on all three rods was assembled and made vacuum tight. The resonator geometry was close to that used in the 10 kW tube. Ten watts of rf power (the maximum available) were absorbed in the resonant loss at its resonant frequency without any damage to it. (The insertion loss of the body was used as a gauge to determine whether or not damage had been done to the resonators.) Since the power in a section of helix with resonant loss appears to be absorbed logarithmically with distance, it was concluded that the resonators at the first turn were absorbing 1 W of power each. It was felt that this power level was much higher than that which resonators in a typical tube will be required to absorb.

In addition to this test, a high average power tube was built on RADC Contract No. F30602-76-C-0326 which utilized resonant loss for BWO stability. The tube was operated CW, delivering over 1 kW of power at 6.5 GHz and over 700 W at 5 and 9.5 GHz with complete stability. The resonant loss characteristic was similar to that of Figure 2. Based on the distribution of the resonators and the tube's output power, it would appear that a conservative estimate of the power absorbed by the resonators closest to the output is 10 W. These data would suggest that the power handling capability of resonant loss is adequate for nearly any application although the exact power handling limit is not known.

XI. TEMPERATURE EFFECTS

The resonant frequency of a resonator changes slightly with temperature. The test body whose insertion loss (measured at room temperature) is shown in Figure 2 was heated to 200°C. The resonant loss characteristic moved down in frequency by 180 MHz. This change is in the "right" direction in the sense that it will cause more loss to be introduced at the BWO frequency. It will however increase the in-band loss slightly.

The same test body was thermally cycled between 60°C and 200°C. The cycle period was two hours and the total cycling time was one week. The insertion loss of the body was measured both before and after the cycling and was unchanged after the cycling.

XII. CONCLUDING REMARKS

The previous ten sections have discussed some of the electrical and mechanical properties of resonant loss. As a result of the work performed on this program, it is now possible to fabricate resonant loss on boron nitride. Furthermore, the important in-band effects of resonant loss have been fairly well characterized. Equally important, with the information gained from the mapping experiment, resonator geometries can be chosen to give the desired resonant frequency with good accuracy. Clearly all of this knowledge will assist in the successful implementation of resonant loss.

Probably the most important conclusion arising from the work performed during this program is that the peak output power of PPM focused, conduction cooled, helix TWTs is no longer limited by BWO if resonant loss is used.

The implications of resonant loss for helix TWT performance appear to be equally dramatic. For the first time since the invention of the helix TWT, high power tubes can be designed solely for optimum in-band performance. In recent years, many studies have been made which indicate that the performance characteristics of present helix TWTs, especially efficiency and bandwidth, can be improved by various methods, such as large pitch steps or tapers, pitch-diameter changes, and dispersion control. It was not possible, however, to implement such schemes without compromising them with additional circuit changes for the purposes of stability. With the advent of resonant loss, these advanced performance schemes can now be implemented without modification.

XIII. SUGGESTIONS FOR FURTHER WORK

It is felt that a good understanding of the basic properties of resonant loss is now in hand. There are several areas in which further work could be done in order to improve and define the performance characteristics of resonant loss. These would include the following:

1. Loss Characteristics (Q)

Resonant loss with more selectivity (higher Q) would be desirable, especially for I-J band tubes.

2. Peak Power Limit

From the measured loss densities provided by resonant loss, it would appear that the peak power limit imposed by BWO would no longer apply. Thus it would be desirable to build an even higher peak power tube than was built during this program.

3. Life Tests

Life tests of resonant loss in operating tubes should be conducted.

REFERENCES

1. Hobrecht: "Resonant Loss for Helix Traveling Wave Tubes." Presented at 1977 IEDM, Washington, D.C., December 1977.
2. Espinosa, Harper: "Helix TWTs for 10 to 25 Kilowatt Peak Power over Octave Bands." Presented at 1974 IEDM, Washington, D.C. December 1974.
3. Harper, Wong, Zavadil: U.S. Patent 3,761,760, September 25, 1973, "Circuit Velocity Step Taper for Suppression of Backward Wave Oscillation in Electron Interaction Devices".